

STRUCTURE SENSITIVITY OF SELECTIVE CO OXIDATION OVER PRECIOUS  
METAL CATALYSTS

A THESIS SUBMITTED TO  
THE GRADUATE SCHOOL OF NATURAL AND APPLIED SCIENCES  
OF  
MIDDLE EAST TECHNICAL UNIVERSITY

BY

BORA ATALIK

IN PARTIAL FULFILLMENT OF THE REQUIREMENTS  
FOR  
THE DEGREE OF MASTER OF SCIENCE  
IN  
CHEMICAL ENGINEERING

FEBRUARY 2005

Approval of the Graduate School of Natural and Applied Sciences

---

Prof. Dr. Canan Özgen  
Director

I certify that this thesis satisfies all the requirements as a thesis for the degree of Master of Science.

---

Prof. Dr. Nurcan Baç  
Head of Department

This is to certify that we have read this thesis and that in our opinion it is fully adequate, in scope and quality, as a thesis and for the degree of Master of Science.

---

Prof. Dr. Şinasi ELLİALTIOĞLU  
Co-supervisor

---

Prof. Dr. Deniz ÜNER  
Supervisor

Examining Committee Members

Prof. Dr. Serpil TAKAÇ

Prof. Dr. Deniz ÜNER

Prof. Dr. Şinasi ELLİALTIOĞLU

Asist. Prof. Dr. Halil KALIPÇILAR

Dr. N. Alper TAPAN

I hereby declare that all information in this document has been obtained and presented in accordance with academic rules and ethical conduct. I also declare that, as required by these rules and conduct, I have fully cited and referenced all material and results that are not original to this work.

Name, Last name : Bora Atalık

Signature :

## **ABSTRACT**

### **STRUCTURE SENSITIVITY OF SELECTIVE CO OXIDATION OVER PRECIOUS METAL CATALYSTS**

Atalık, Bora

M.S., Department of Chemical Engineering

Supervisor: Prof. Dr. Deniz ÜNER

February 2005, 72 pages

In this study, the effect of Pt particle size on the reaction rate and selectivity of preferential oxidation of CO (PROX) reaction was investigated on Pt/Al<sub>2</sub>O<sub>3</sub>. 2% Pt/γ-Al<sub>2</sub>O<sub>3</sub> catalysts were prepared by incipient wetness method; the particle size of the catalysts was modified by calcination temperature and duration. Therefore, the relative amounts of low and high coordination atoms on the metal particle surface can be changed. Over these catalysts, first, the CO oxidation reaction was studied in the absence of hydrogen. The catalyst having the highest dispersion, i.e., lowest metal particle sizes, had the highest activity as indicated by its lowest light-off temperature. On the other hand, the turnover frequencies (TOF) of the catalysts were increasing with

decreasing dispersion. The activation energy of the catalysts were also compared and examined: as the particle size increased, the activation energy decreased. In the second part, preferential oxidation of CO reaction in the presence of hydrogen was studied. Both CO conversion and selectivity first increased with increasing reaction temperature, then exhibited a maximum, and finally decreased. Both CO conversion and selectivity did not show any trend for different dispersed catalysts for  $\lambda \left( 2 \frac{P_{O_2}}{P_{CO}} \right)$  was 1. In order to reach a definite conclusion about the structure sensitivity of selective CO oxidation, the experiments with different  $\lambda$ 's and space times over the same catalysts should be performed.

**Keywords:** PROX, CO oxidation, Structure Sensitivity, Catalysis, Precious Metals, Pt

## ÖZ

### SEÇİCİ CO OKSİDASYONUNUN DEĞERLİ METAL KATALİZÖRLER ÜZERİNDE YAPISAL DUYARLILIĞI

Atalık, Bora

Yüksek Lisans, Kimya Mühendisliği

Tez Yöneticisi: Prof. Dr. Deniz Üner

Şubat 2005, 72 sayfa

Bu çalışmada, Pt/Al<sub>2</sub>O<sub>3</sub> katalizörü üzerinde platinyum parçacık büyüklüğünün seçici CO oksidasyonunun reaksiyon hızı ve seçiciliğine olan etkisi çalışılmıştır. Islaklık başlangıcı metoduyla hazırlanan 2% Pt/γ-Al<sub>2</sub>O<sub>3</sub> katalizörlerinin metal parça büyüklükleri farklı sıcaklıklarda ve sürelerde kalsine edilerek değiştirilmiştir. Bu sayede, metal parçacık yüzeyindeki düşük ve yüksek koordinasyonlu atomların oranları değiştirilebilmiştir. İlk olarak, bu katalizörler üzerinde hidrojeniz ortamda CO oksidasyonu reaksiyonu çalışılmıştır. En aktif katalizörün metal dağılım oranı en yüksek olan katalizör (metal parçacık büyüklüğü en küçük olan katalizör) olduğu görülmüştür. Ancak devir-daim sıklıklarına bakıldığında, metal dağılım oranı düştükçe devir-daim sıklığının arttığı gözlemlenmiştir. Ayrıca reaksiyonun değişik katalizörler üzerinde aktivasyon enerjileri incelenmiş ve metal parçacık büyüklüğü arttıkça aktivasyon enerjisinin azaldığı gözlemlenmiştir. Çalışmanın ikinci bölümünde, hidrojenli ortamda seçici CO oksidasyonu reaksiyonu incelenmiştir.

Başlangıçta, hem karbon monoksit yüzde dönüşümü, hem de karbon monoksit seçiciliğinin sıcaklıkla beraber arttığı, daha sonra karbon monoksit yüzde dönüşümü ve seçiciliğinin maksimum değere ulaştığı ve son olarak sıcaklık arttıkça azaldığı tespit edilmiştir. Farklı metal dağılım oranlı katalizörler için, karbon monoksit ve oksijenin stokiyometrik olarak kullandıkları durumda karbon monoksit dönüşümü ve seçiciliği herhangi bir eğilim göstermemiştir. Seçici karbon monoksit oksidasyonu reaksiyonunun yapısal duyarlılığı hakkında kesin bir yargıya varabilmek için, aynı katalizörler üzerinde değişik CO/O<sub>2</sub> oranlarında ve alıkonuş zamanlarında deneyler gerçekleştirilmesi gerekmektedir.

**Anahtar Kelimeler:** Tercihli karbon monoksit oksitlenmesi, CO oksitlenmesi, Yapısal Duyarlılık, Katalizör, Değerli Metaller, Pt

To My Family,



## **ACKNOWLEDGEMENTS**

I would like to thank my supervisors Prof. Dr. Deniz ÜNER and Prof. Dr. Şinasi Ellialtıođlu for their valuable support, encouragement, patience and guidance, for their kind attitude throughout this study.

I would also like to thank all the members of CAC-TUS group, past and present.

I am grateful for the financial support for this project provided by TÜBİTAK under research grant number of MISAG-188.

I am grateful for the assistantship provided by METU Graduate School of Natural and Applied Sciences.

## TABLE OF CONTENTS

PLAGIARISM.....	iii
ABSTRACT.....	iv
ÖZ.....	vi
DEDICATION.....	viii
ACKNOWLEDGEMENTS.....	ix
TABLE OF CONTENTS.....	x
LIST OF TABLES.....	xii
LIST OF FIGURES.....	xiii
NOMENCLATURE.....	xv
CHAPTER	
1. INTRODUCTION.....	1
1.1 PROX Reaction.....	1
1.2 Structure Sensitivity.....	3
2. LITERATURE SURVEY.....	8
2.1 Competitive Adsorption and Reaction of CO, H <sub>2</sub> and O <sub>2</sub> on Single Crystal Surfaces.....	9
2.2 CO Oxidation Over Supported Catalysts.....	15
2.3 Selective CO oxidation.....	21
3. EXPERIMENTAL.....	26
3.1 Catalyst Preparation.....	26
3.2 Characterization of Catalysts.....	26
3.3 Activity measurements.....	27
3.4 Isothermal CO Oxidation Reactions.....	30

4. RESULTS AND DISCUSSION.....	31
4.1 The Structure Sensitivity of CO Oxidation.....	31
4.1.1 Light-off Performances of Catalysts.....	32
4.1.2 Turnover frequencies of CO oxidation over different catalysts.....	34
4.1.3 Apparent activation energies of CO oxidation over different catalysts.....	37
4.1.4 Structure sensitivity of PROX reaction .....	38
4.2. Preferential oxidation of CO (PROX) reaction.....	41
4.2.1 CO oxidation in the absence of H <sub>2</sub> .....	41
4.2.2 CO oxidation in the presence of H <sub>2</sub> .....	43
5. CONCLUSION.....	53
RECOMMANDATION.....	54
REFERENCES.....	55
APPENDICES.....	63
A. Volumetric Chemisorption.....	64
B. Calculations.....	66
C. Isothermal CO Oxidation Performances of 2% Pt/ $\gamma$ -Al <sub>2</sub> O <sub>3</sub> Catalysts.....	71

## LIST OF TABLES

2.1. The adsorption energy of CO on terrace and edge sites of catalysts.....	11
2.2. The activation energies and reaction orders for various platinum catalysts.....	18
2.3. The maximum conversions and selectivities of selective CO oxidation reaction.....	24
4.1 The activation energies of CO oxidation reaction with respect to dispersion and particle size of catalysts.....	38
4.2. The $T_{50}$ 's which were obtained by using both GC and MS for all catalysts.....	39
4.3 The ignition temperatures of PROX reactions over 2% Pt/ $\gamma$ - $Al_2O_3$ catalysts in the presence and absence of hydrogen.....	45
A.1. Dispersion values of 2% Pt/ $Al_2O_3$ calcined at different temperatures and durations.....	64
C.1 The reaction orders of CO and $O_2$ for CO oxidation reaction.....	71

## LIST OF FIGURES

1.1 The structure of the cuboctahedron shape.....	5
1.2 The change in fraction of low and high coordination atoms to the total number of surface atoms with respect to approximate particle diameter (Strohl and King).....	5
1.3 The change in dispersion with respect to approximate particle diameter (Strohl and King).....	6
3.1 Home built multi-port high-vacuum Pyrex glass manifold.....	27
3.2 The experimental setup.....	29
4.1 The light-off curves of the catalysts with different dispersions.....	33
4.2 The turnover frequencies of samples with different dispersions with respect to temperature.....	35
4.3 The maximum and minimum differences between $T_{50}$ data obtained by gas chromatograph and mass spectrometer (a) $d=0.29$ , (b) $0.04$ .....	40
4.4 The light-off curves of the catalysts for various dispersions.....	42
4.5 The turnover frequencies of samples with changing dispersions with respect to temperature.....	43
4.6 The oxygen conversion of samples with changing dispersions with respect to temperature.....	44
4.7 The CO conversion of samples with changing dispersions with respect to temperature.....	47
4.8 The selectivity for CO oxidation of samples with changing dispersions with respect to temperature.....	47
A.1. $H_2$ adsorption isotherm of 2% Pt/ $\gamma$ - $Al_2O_3$ with dispersion of 0.83.....	64
B.1 $\ln(\text{rate})$ vs. $T^{-1}$ plot of 2% Pt/ $Al_2O_3$ catalysts which dispersion is 0.04....	68

B.2 The reaction orders of the reaction over the catalyst with dispersion of  
0.63) (a) CO order,  $P_{O_2} = 41.5$  Torr and  $P_{CO} = 5.3-9.6$  Torr ; (b)  $O_2$  order,  
 $P_{CO} = 55.4$  Torr and  $P_{O_2} = 6.1-8.5$  Torr.....70

## NOMENCLATURE

$d$	Dispersion (dimensionless)
$E_a$	Activation energy (kJ/mole)
$F_i$	Molar flow rate of species $i$ (mole/s)
$F_{i_0}$	Molar flow rate of species $i$ at the inlet of the reactor (mole/s)
$k$	Reaction rate constant ( $s^{-1}$ or $mol/g \text{ cat} \cdot s^{-1}$ )
$m_{cat}$	Weight of catalyst (g)
$M_{Pt}$	Molecular weight of platinum (g/gmol)
$N_{Av}$	Avagadro number (# of atoms/moles)
$N_i$	Number of moles of species $i$ (mole)
$ps$	Particle size
$P_i$	Partial Pressure of component $i$ (Torr)
$Pt$	Platinum
$R$	Ideal gas constant (J/mol.K)
$T$	Temperature (K)
$r_i$	Reaction rate of species $i$
$SD$	Active site density
$X_i$	Conversion of species $i$ (%)
$W_{Pt}$	Platinum content of catalyst (wt %)

## **CHAPTER 1**

### **INTRODUCTION**

#### **1.1. PROX Reaction**

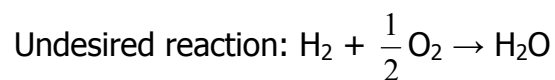
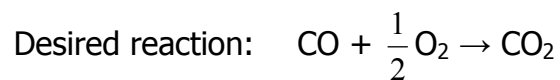
The selective oxidation of CO in a H<sub>2</sub>-rich atmosphere (PROX) has long been of considerable technical interest for purification of hydrogen feed gas, e.g., for H<sub>2</sub> supply in ammonia synthesis. Over the last two decades, the PROX process has attracted new interest due to its use in fuel cell technology.

H<sub>2</sub> fueled, polymer electrolyte membrane fuel cells (H<sub>2</sub>-PEMFC) are highly advantageous with respect to current conventional internal combustion engines due to production of electricity without polluting the environment. Since pure hydrogen is the ideal fuel for H<sub>2</sub>-PEMFC, the use in vehicle applications is faced with serious problems associated with the distribution and storage of hydrogen. A promising way to overcome these problems is to produce the hydrogen feed gas on-board, in a fuel-processing unit, by converting a conventional fuel such as natural gas, gasoline or methanol to a H<sub>2</sub>-rich gas mixture. The catalytic steam reforming of methanol or partial oxidation of gasoline can be used for production of hydrogen. In either case, the resulting gas mixture contains significant amounts of CO and it is further processed in a water gas shift reactor. In this way the gas stream becomes richer in H<sub>2</sub> and it is composed of 40-75% H<sub>2</sub>, 15-20% CO<sub>2</sub>, ~10% H<sub>2</sub>O, 0-



25% N<sub>2</sub> and 0.5-1% CO (Manasilp and Gulari, 2002). Unfortunately, even this low CO concentration cannot be tolerated by the H<sub>2</sub>-PEM fuel cells. The H<sub>2</sub>-PEM fuel cell's anode uses a Pt catalyst, which is very sensitive to CO poisoning at its low operating temperatures. Thus it is crucial to purify further the hydrogen feed gas reducing the CO concentration below 10 ppm (Igarashi et al., 1995).

Available methods of CO removal from H<sub>2</sub>-rich atmospheres are the use of palladium or Pd-alloy membranes, catalytic methanation and selective catalytic CO oxidation. Selective CO oxidation is the most straightforward, simpler, and cost effective method. However, the hydrogen oxidation competes with CO oxidation leading to the loss of the fuel efficiency. So, the catalyst of PROX reaction should fulfill the following important requirements: 1) to possess high CO oxidation activity, 2) to exhibit high selectivity with respect to the undesired H<sub>2</sub> oxidation (ideally, the catalyst should be inactive for H<sub>2</sub> oxidation in order to avoid losses of fuel hydrogen), 3) to function at the temperature window defined by the temperature level of the fuel-processing unit (250-300°C) and that of the H<sub>2</sub>-PEMFC (80-100°C) (Avgouropoulos et al., 2002).



A number of catalysts have been investigated for the selective CO oxidation in excess hydrogen gas stream. Some of the most effective ones include supported precious metals such as Pt, Ru, Rh, and Au.

## 1.2. Structure Sensitivity

Most of the adsorption processes and surface reactions occur only on special sites that are called as active sites. The idea that there are active sites implies that reaction rates vary with surface structure. In 1960s Boudart classified the surface reactions in two general classes; structure sensitive reactions and structure insensitive reactions (Masel, 1996). If rate of surface reaction varies with surface crystal orientation, these reactions are called structure sensitive reactions. However, if reaction rate is not varying with surface structure, these reactions are called structure insensitive reactions.

There are two ways to understand whether a reaction is structure sensitive or not. One of the earliest ways is to observe the variation of the reaction rate with particle size on a supported catalyst. Another way is to run reactions on a variety of faces of single crystals and look for a variation in rate with crystal orientation. These experiments are performed under ultrahigh vacuum (UHV) conditions.

Over the years, there have been several models proposed to understand the nature of structure sensitive reactions. So far, two basic models were postulated as geometric (ensemble) effects and electronic (ligand) effects.

Geometric (ensemble) effect requires correct number and coordination of surface atoms for a certain reaction to occur. On the other hand, electronic (ligand) effect requires the sites to have the correct electronic configuration to result in a given adsorbate-adsorbent bond strength.

Furthermore, thermodynamic effects are also important in variation of the rates of reactions on surface. Heat of adsorption and desorption of the intermediates of a reaction can vary significantly with crystal face. Generally,

the heat of adsorption of gases on the stepped surfaces is higher with respect to flat planes. So, this means that the stepped surfaces bind intermediates more strongly than flat planes. This is expected to cause a variation in the rate of reaction. Since the stepped sites bind intermediates more strongly, the reactivity of these intermediates will be less. Consequently, the surfaces that bind intermediates less strongly will have the higher activity.

In past, CO oxidation reaction is usually classified as a structure insensitive reaction (Berlowitz et al., 1988, Ladas et al., 1981). However, recent studies (Zafiris and Gorte, 1993, Gracia et al., 2003) revealed that the reaction rate per surface atoms was increasing with increasing particle size or decreasing dispersion.

The particles of supported metal catalysts generally form cuboctahedron shapes (depending on their surface free energies) given in Figure 1.1. There are primarily two types of surface sites of metal particles: these are low coordination sites (edge and corner atoms), and high coordination sites (terrace or flat plane atoms). There are two types of terrace sites with different crystallographic orientation. These are given as terrace (111) and terrace (100) in Figure 1.2. In addition to these sites, there are also bulk atoms inside the particles of catalysts, which are not accessible therefore catalytically not important. According to the studies of Strohl and King, and Schimpf et al. (2002), it was found that the proportions of the low and high coordination atoms on the surface were significantly changing with particle diameter. The fraction of low coordination atoms (edge and corner atoms) with respect to total surface atoms was considerably decreasing with increasing particle diameter. On the other hand, the fraction of high coordination atoms (terrace or flat plane atoms) was increasing with increasing particle diameter as it is given in Figure 1.2.



**Figure 1.1** The structure of the cuboctahedron shape

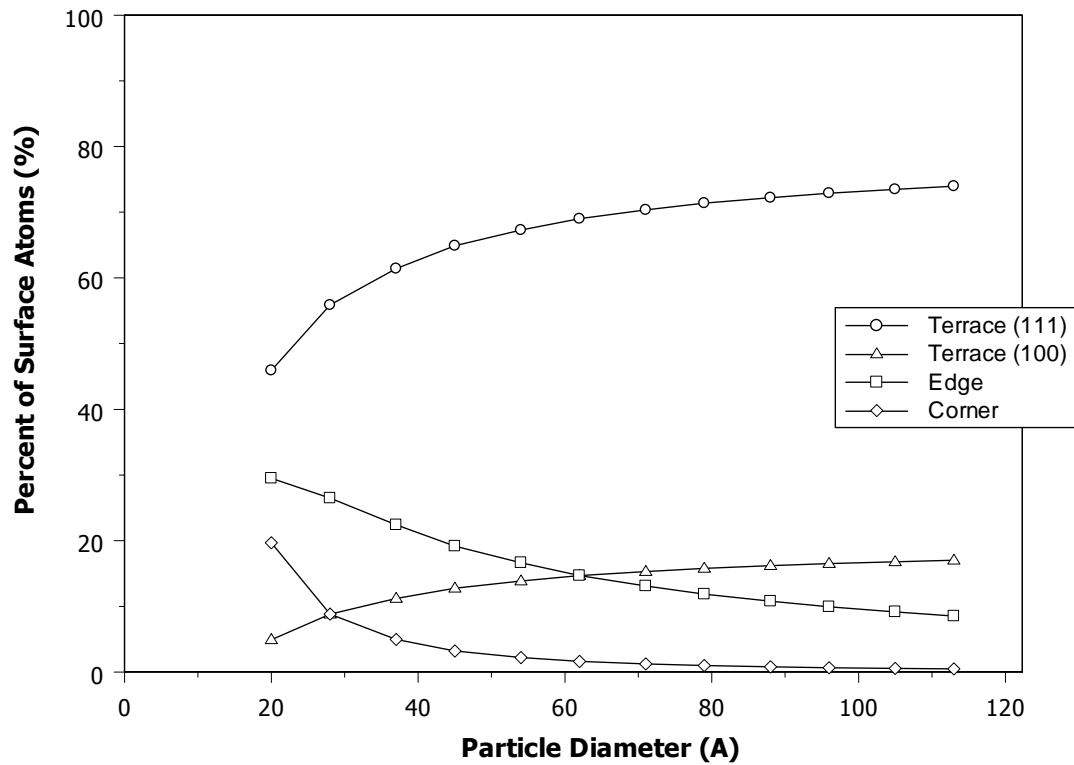


**Figure 1.2** The change in fraction of low and high coordination atoms to the total number of surface atoms with respect to approximate particle diameter (Strohl and King, personal communication)

As one can easily deduce from the data presented in Figure 1.2, by changing metal particle diameter, the relative population of low coordination (edge and corner) and high coordination (100 and 111 terraces) atoms can be changed. If this can be done in a controlled fashion, structure sensitivity of a reaction can be followed on powdered catalysts.

The dispersion of the catalysts can be modified by changing the calcination temperature during the catalyst preparation. The dispersion can be defined as the ratio of the surface atoms to the total number of atoms. According to the study of Strohl and King, as the particle diameter of cuboctahedron structure was increased, the dispersion of that structure decreased (Figure 1.3).

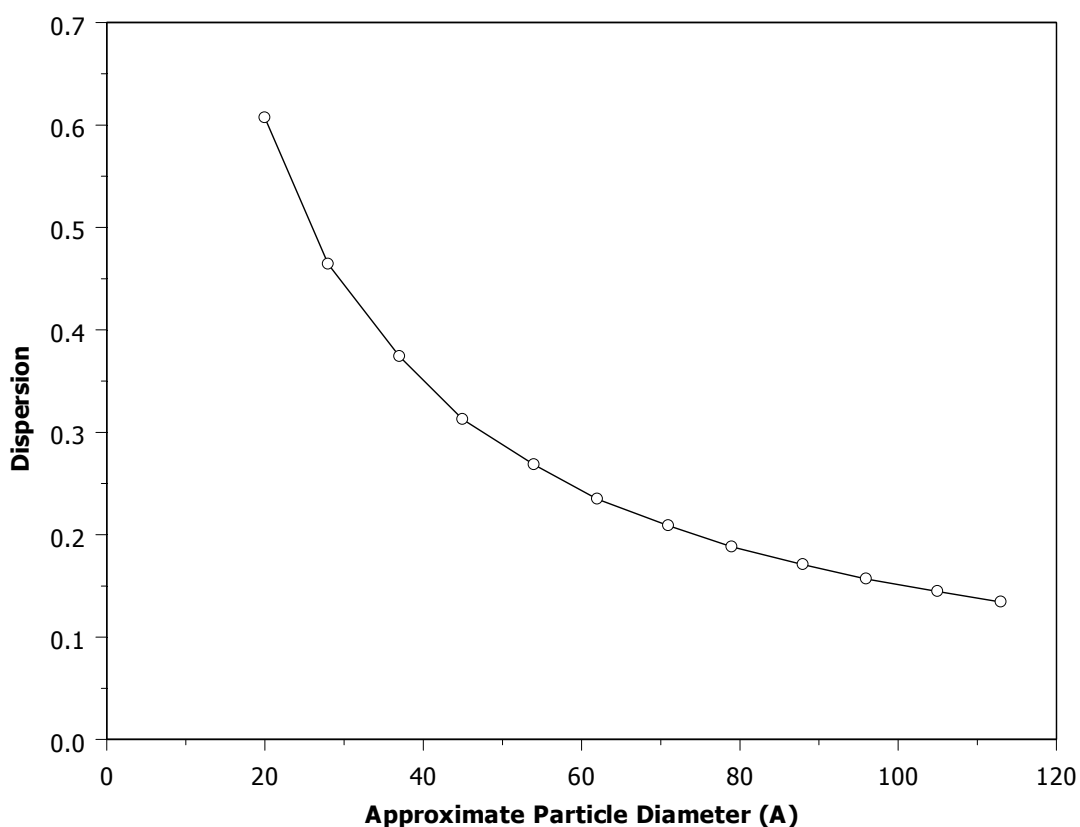


**Figure 1.3** The change in dispersion with respect to approximate particle diameter (Strohl and King, personal communication)

Pt and Pd like precious metals are generally used to convert CO to CO<sub>2</sub> in exhaust emissions and to remove CO again in hydrogen-rich mixtures that are used for the feed to fuel cells. Because of the high prices of these precious metals (approximately 500\$/ounce), they have to be used in high efficiency. So, it is highly important to find which particle diameter of the platinum catalyst give optimal performance.

In this study, the objective was to find out whether selective CO oxidation reaction was structure sensitive. First step of the study was to observe the structure sensitivity of CO oxidation reaction in the absence of hydrogen. In order to observe the structure sensitivity, first the catalysts with different particle sizes were prepared. The light-off performances, the specific rate of reaction and activation energies of the reactions over the catalysts with different particle size were compared for CO oxidation. Then, the CO conversion and selectivity data of CO oxidation in the presence of hydrogen were obtained and the structure sensitivity of selective CO oxidation reaction was discussed.

## **CHAPTER 2**

### **LITERATURE SURVEY**

The reaction between hydrogen, carbon monoxide and oxygen has drawn much attention in the past due to the fundamental nature of the interaction on the supported metal surfaces. Furthermore, hydrogen and carbon monoxide are used as characterization adsorbents for supported metals. For this reason there is a vast amount of literature on adsorption of especially hydrogen and carbon monoxide, both on supported metals and on single crystal surfaces. The literature review of this thesis is organized in the following manner. First, the experimental single crystal literature will be summarized from the point of view of the adsorption of hydrogen oxygen and carbon monoxide. It is almost impossible to collect all the literature in this work. Therefore, the articles covering the nature of adsorption of all three adsorbents over the same substrate were selectively collected. Then, the literature on PROX reaction over supported metals will be presented.

## 2.1. Competitive Adsorption and Reaction of CO, H<sub>2</sub> and O<sub>2</sub> on Single Crystal Surfaces

Gland et al. (1983) studied the adsorption of CO and oxygen and CO oxidation on kinked Pt(321) surface by using HREELS, TPR and titration of adsorbed atomic oxygen by CO. They observed that atomic oxygen adsorbed on step sites is the dominant form of adsorbed oxygen at low coverages. Thermal desorption spectra of CO from the clean (321) surface indicated that CO preferentially adsorbed on terraces corresponding to step sites. They also studied the coadsorption of CO and oxygen. They found that an adsorbed layer of oxygen does not completely inhibit CO adsorption. However, no oxygen adsorption occurs as indicated by the absence of CO<sub>2</sub> and oxygen desorption in TPR experiment, if the (321) surface is first saturated with CO. They also found that CO<sub>2</sub> formation begins at lower temperature on the (321) surface than on the (111) surface, which indicates that lower energy pathways are available on (321) surface. When they covered the surface with oxygen and gave a small amount of CO, they observed that the atomic oxygen adsorbed on terraces reacts preferentially with CO (TPR). The same result was obtained by titration of adsorbed atomic oxygen by CO. Another conclusion is that CO adsorbed on terraces reacts more rapidly than CO adsorbed along the rough step sites.

Intermediate conclusion: CO adsorbed on terraces reacts more rapidly than CO adsorbed at rough edges. At low coverages oxygen adsorbs in molecular form, at step edges.

Luo et al. (1992) studied CO adsorption on Pt(335) at various coverages using TPD and EELS. They found that at low CO coverage, edge sites were favored, with edge atop sites filling first, followed by edge bridge sites. The edge structure was stabilized when  $2/3^{\text{rd}}$  of the edge sites are filled, with



equal concentrations of bridge and atop CO. As terrace sites began to fill, terrace CO adsorbed on atop sites until  $1/3^{\text{rd}}$  of the terrace sites were filled. After that, terrace adsorption occurred on bridge sites. Simultaneously, CO adsorbed on edge atop sites, displacing the existing bridge CO. At saturation, the edge was fully saturated with atop CO,  $1/2$  of the terrace sites are occupied and the ratio of atop to bridge CO on the terrace was 2:1. They also estimated the activation energies for CO desorption from edge and terrace sites. The activation energy of desorption for edge and terrace CO was given in Table 2.1.

Intermediate conclusion: at low coverages, bridge bonded CO is the preferred type; at high coverages, atop adsorption starts to dominate. CO adsorption starts from edge sites then the terraces are filled.

A comparative investigation of oxygen adsorption on Pt(111) and Pt(112) was performed by Winkler et al. (1988). They measured the sticking coefficients for both surfaces. On Pt(112) the initial sticking coefficient,  $s_0$ , was 0.97 and remains constant in the low coverage regime for molecular oxygen. For Pt(111), where  $s_0=0.29$ , an increase of the sticking coefficient at low coverage indicates an enhanced adsorption probability in the vicinity of single adsorbed oxygen molecules. For atomic oxygen the initial sticking coefficients were 0.05 and 0.53 for Pt(111) and Pt(112), respectively. The saturation coverage of oxygen on Pt(111) was found to be 0.5 and 0.25 at 87 K and 300 K, respectively. For Pt(112) they obtained 0.51 and 0.37 at 87 K and 300 K, respectively, indicating a higher dissociation probability at step sites with regard to that at terrace sites.

Intermediate conclusion: as the defect site concentration on a catalyst increases, the sticking coefficient and saturation coverage of oxygen increased.

**Table 2.1.** The adsorption energy of CO on terrace and edge sites of catalysts

<b>Catalysts</b>	<b>E<sub>d</sub> of Terrace Sites (kJ/mol)</b>	<b>E<sub>d</sub> of Edge Sites (kJ/mol)</b>	<b>References</b>
Pt(111)	123.8	–	McCabe and Schmidt (1977)
Pt(111)	113.0	–	Collins and Spicer (1977)
Pt(111)	133.9	–	Ertl et al. (1977), Poelsema et al. (1984), Seebauer et al. (1986)
Pt(S)[6(111)x(100)]	113.0-100.4	138.1	Collins and Spicer (1977)
Pt(112) Pt(S)[3(111)x(100)]	119.2-94.0	147.3	McCabe and Schmidt (1977)
Pt(321)	96	151	McClellan et al. (1981)
Pt(335)	114.6-97.5	133.9-119.2	Luo et al. (1992)

The interaction of co-adsorbed CO and H<sub>2</sub> on the steps of Pt(112) [Pt(S)[3(111)\*(001)]] was examined by using ESDIAD, LEED and TPD by Henderson and Yates (1992). They observed that defects on Pt increased the hydrogen sticking coefficient and H atoms bind more strongly at Pt defect sites than on terraces. In addition to that as 0.05 ML H adsorbed on 0.16 ML CO covered Pt(112), the CO molecular orientation on step sites was altered. Hydrogen exerted a repulsive interaction on CO which caused CO migration on the step edge to ultimately form close-packed CO arrays resulting in one-dimensional CO island formation. As a similar result, CO nucleation and

island formation on the steps also occurred on the H saturated Pt(112) surface, and that was causing H displacement from the 4-fold step sites to terraces.

Wang et al. (1995) studied co-adsorbed CO and H on the stepped Pt(335) [Pt(S)[4(111)\*(100)]] surface with EELS and TPD. Similar with other studies both CO and H adsorbed on step sites at low coverages individually. At higher coverages they began to occupy the terrace sites. As a result of co-adsorbed CO and H experiments on the step edges, they observed that co-adsorbed H shifted CO from atop to bridge sites. At the highest hydrogen coverage, the atop peak of CO was reduced to about 25% of its original intensity. Another observation about the co-adsorption of CO and H was that as the temperature was increased for TPD, CO became mobile and replaced hydrogen atoms at the edge sites. If there is enough CO to fill all the edge sites then no hydrogen desorption from edge sites was observed. They also found that CO and H did not segregate on Pt(335) terraces and hydrogen adsorption had no effect on CO atoms adsorbed on terrace sites.

Szabo et al. (1992) studied the co-adsorption of oxygen and carbon monoxide on the stepped Pt(112) surface by using ESDIAD, TPD and LEED. For CO coverages,  $\theta_{CO} < 0.17$  ML, CO adsorbed on the step edge sites of the Pt(112). As full coverage was approached, terrace sites were also populated and a final CO saturation coverage of 0.79 ML could be achieved. It was also found that atomic oxygen species were chemisorbed preferentially at step sites and after desorption of all the adsorbed oxygen, there was no evidence for Pt reconstruction, CO adsorbed on the terraces when chemisorbed oxygen blocks step sites for adsorption at 90 K, in the case of adsorption of CO on the O/Pt(112). After annealing the CO/O/Pt(112) system to 230 K, CO migrates to the step-edge sites. These measurements clearly showed that CO preferentially adsorbed on sites not bonded to oxygen atoms. For CO<sub>2</sub>

production the surface was preadsorbed by 0.18 ML oxygen. There was no CO desorption from the CO/O/Pt(112) until a CO coverage of about 0.19. Below that coverage, the entire adsorbed CO desorbed as CO<sub>2</sub>. Above that coverage, CO desorption increased linearly with increasing CO coverage and CO<sub>2</sub> production leveled off. In addition to that, the CO sticking coefficient was the same for both CO+O/Pt(112) and CO/Pt(112) systems in this coverage range indicating that preadsorbed oxygen did not lead to any significant decrease of the CO sticking coefficient. They also found that the CO isotope adsorbed on terrace sites is exclusively oxidized at a lower temperature than CO bound at step sites, suggesting that CO oxidation is easier at terrace sites, compared to step sites.

Intermediate conclusion: CO oxidation is easier on terrace sites than on edge sites. Oxygen and CO do not compete for the same type of sites.

Xu and Yates(1993) used IRAS and TPR in order to identify the most active catalytic sites on a Pt(335) crystal which has four-atom wide terraces of (111) orientation separated by single atom steps of (100) orientation. They found that CO preferentially adsorbs on the step sites at low coverage. As the CO coverage is increased, terrace CO develops and finally reaches saturation coverage. Chemisorbed oxygen is also adsorbed on step sites and the adsorption of oxygen atoms on the step sites blocks CO adsorption. CO initially adsorbed on step sites is displaced by O(a) to produce terrace CO. They also examined that chemisorbed CO on terrace sites is more easily oxidized, compared to CO on the step sites. On the other hand, oxygen atoms adsorbed on step sites are more reactive than terrace oxygen atoms. They suggested that the most favorable reaction sites at high CO coverages for the oxidation of CO involve CO species adsorbed on terrace sites adjacent to O species adsorbed on step sites.

The reaction site for carbon monoxide oxidation on a stepped Pt(113) surface was studied with angle-resolved thermal desorption by Yamanaka et al. (1997). They observed that the preference of the reaction site switches from the (100) step to the (111) terrace around  $\theta_{\text{CO}}$  close to  $\theta_0$  with increasing  $\theta_{\text{CO}}$ . The variation of the oxygen coverage affected the site switching much less than that of CO and increase in oxygen coverage enhances the reaction rate on the step. They suggested that the site switching with increasing  $\theta_{\text{CO}}$  was caused by the repulsive force of CO on step platinum atoms towards oxygen. This fact occurred around  $\theta_{\text{CO}} = \theta_0$  suggested that two CO ad molecules on step atoms are required to repel an oxygen adatom to the terrace.

Carbon monoxide oxidation had been studied by Burnett et al. (2004), using in situ soft X-ray techniques and ultrahigh vacuum (UHV) temperature-programmed reaction spectrometer (TPRS), on a well-characterized supported platinum thin film. CO and O<sub>2</sub> temperature-programmed desorption (TPD) experiments indicated that the Pt film surface was similar to Pt(111), but with a higher defect site concentration. Unlike with the Pt(111) surface, the onset temperature for oxidation of a saturated coverage of CO on the platinum thin film decreased dramatically with increasing oxygen pressure. The CO oxidation onset temperature decreased from 340 K in  $1 \times 10^{-5}$  Torr of flowing oxygen to 230 K in  $1 \times 10^{-2}$  Torr of flowing oxygen. Therefore, oxidation was not limited by CO desorption for high CO coverages, and reactions at defect sites controlled the rate of CO oxidation at high oxygen pressures.

Intermediate conclusion: the reactions at defect sites controlled the rate of CO oxidation at high oxygen pressures.

Engstrom and Weinberg (1988) investigated the oxidation of CO on Pt(110) surface by using STM. They found that there was a strong correlation between the magnitude of the activation energy of reaction and the coverage of oxygen adatoms. A decrease in the magnitude of the activation barrier was observed as the fractional coverage of oxygen increased above approximately 0.15. The activation energy varied between approximately 33 and 92 kJ/mol. The local configuration of the reactants played crucial role in determining the surface reaction dynamics. At relatively high oxygen coverages ( $\theta_o \geq 0.15$ ), adsorbed CO reacted in regions of high local oxygen adatom concentration. In these regions of the surface, the adsorbed reactants had reduced binding energies that lead directly to a decrease in the activation energy for the production of CO<sub>2</sub>.

## **2.2. CO Oxidation Over Supported Catalysts**

Studies of carbon monoxide oxidation on the platinum metals previous to 1979 were reviewed by Engel and Ertl (1982). They established that CO oxidation on Pt takes place through Langmuir-Hinshelwood mechanism, where both CO and oxygen are chemisorbed on the surface prior to the reaction. The product CO<sub>2</sub> desorbs instantaneously after the reaction. Since adsorbed CO is known to be substantially more mobile than adsorbed atomic oxygen, the primary reaction path must involve CO surface diffusion up to largely immobile adsorbed oxygen atoms. The activated complex is formed as the CO approaches the oxygen.

The dependence of specific rate of CO oxidation Pt particle size was first observed by McCarthy et al. (1975) on 0.035% Pt/ $\alpha$ -Al<sub>2</sub>O<sub>3</sub>. They found that specific rate was higher for low dispersed catalyst than for highly dispersed

Pt catalysts in the range of low CO partial pressure while at higher CO partial pressure, specific rate was relatively insensitive to particle size.

Zafiris and Gorte (1993) investigated the catalytic CO oxidation on Pt/ $\alpha$ -Al<sub>2</sub>O<sub>3</sub>(0001) and looked for whether this reaction shows structure sensitivity or not. They prepared the catalysts by vapor deposition of Pt on  $\alpha$ -Al<sub>2</sub>O<sub>3</sub>(0001) and used two metal coverages,  $5 \times 10^{15}$  Pt/cm<sup>2</sup> and  $0.25 \times 10^{15}$  Pt/cm<sup>2</sup>. For these coverages, the average particle sizes, determined from dispersion measured by CO adsorption, were 14 nm and 1.7 nm, respectively. After they made kinetic experiments, they obtained that there is a discrepancy between the turnover frequencies for 1.7- and 14-nm particle sizes. They have demonstrated that the oxidation of CO by O<sub>2</sub> over Pt is structure sensitive at typical reaction pressures. Changes in the specific rates for small Pt particles compared to larger ones can be explained by the lower desorption rates for CO.

Matsushashi et al. (2004) tried to understand the effect of preparation conditions on the platinum metal dispersion and the effect of dispersion on turnover frequencies (TOF) of several representative reactions, where platinum-supported alumina catalysts were prepared by impregnation methods in which preparation conditions were fixed or not fixed using certain alumina. Catalytic activities for oxidation of CO were compared based on the TOF of these reactions. The researchers obtained inverse correlation between the platinum dispersions and the turnover frequency of CO oxidation reaction. They found that turnover frequency was increasing with decreasing platinum dispersion. In addition to that they also observed that the activation energy of oxidation increased with increasing of platinum dispersion. This trend indicated that the performance of one active site was reduced; the metallic character of platinum particle is being lost as it becomes a smaller particle.

The effect of particle size on the rate of the CO oxidation reaction was examined on Pt/SiO<sub>2</sub> by Gracia et al. (2003). The catalysts were prepared by using two different methods in order to obtain high and low dispersed catalysts with identical Pt loading. They found that the light-off temperature of catalysts which were prepared by wet impregnation method is similar for samples calcined at 400 and 500°C (ca. 170°C). However, for catalyst calcined at 600°C, the light off temperature is about 25 and 50°C higher than those of the other catalysts. In addition to these catalysts, they also prepared prereduced Pt/SiO<sub>2</sub> catalysts. The dispersion of these catalysts was varying from 0.29 to 0.76. The light-off performances of the catalyst were similar but the TOF of the low-dispersion catalyst is the highest. The Arrhenius plot showed that the apparent activation energy decreases as the dispersion of the Pt/SiO<sub>2</sub> catalysts decreases. So, they concluded that CO oxidation on small Pt crystallites is a structure-sensitive reaction.



**Table 2.2.** The activation energies and reaction orders for various platinum catalysts. Rate =  $k \cdot P_{CO}^m \cdot P_{O_2}^n$

Catalyst	T Range (K)	Reactant Composition	Total Flow Rate or Total Pressure	Ea (kJ/mol)	m	n	Ref.
0.04 % Pt/ $\gamma$ -Al <sub>2</sub> O <sub>3</sub>	463-483	CO = 0.5-2 ml/min O <sub>2</sub> = 0.5-2 ml/min	100 ml/min	78	-0.51	0.76	Kim and Lim (2002)
Pt/ $\gamma$ -Al <sub>2</sub> O <sub>3</sub>	463-503	P <sub>CO</sub> = 0.22-8.3 kPa P <sub>O<sub>2</sub></sub> = 0.37-8.3 kPa	110 kPa	112	-1	1	Nibbelke et al. (1997)
0.24 % Pt/ $\gamma$ -Al <sub>2</sub> O <sub>3</sub>	< 473	0.4-1.5 % CO 0.4-1.5 % O <sub>2</sub>	3.5 L/min	55.2	-1.5	1	Muraki et al. (1991)
0.5 % Pt/ $\gamma$ -Al <sub>2</sub> O <sub>3</sub>	423-523	0.02-1.5 % CO O <sub>2</sub> /CO = 0.5-1.5	120 ml/min	71	-0.4	0.8	Kahlich et al. (1997)
2 % Pt/SiO <sub>2</sub>	350-410	1 % CO 10 % O <sub>2</sub> balance He	60 ml/min	55±1 (d=0.26) 72±3 (d=0.63) 92±2.5 (d=0.76)	-	-	Gracia et al. (2003)
Pt/ $\alpha$ -Al <sub>2</sub> O <sub>3</sub> (0001)	560-680	P <sub>CO</sub> = 1-20 Torr P <sub>O<sub>2</sub></sub> = 1-20 Torr	NR	125±12 (ps=14 nm) 172±17 (ps=1.7 nm)	-0.6	1.3	Zafiris and Gorte (1993)

d : Dispersion NR: Not reported

ps : Particle Size

**Table 2.2.** Continued

Catalyst	T Range (K)	Reactant Composition	Total Flow Rate or Total Pressure	Ea (kJ/mol)	m	n	Ref.
0.5 % Pt/ $\gamma$ -Al <sub>2</sub> O <sub>3</sub>	300-750	1 % CO 0.5 % O <sub>2</sub>	NR	134	-	-	Martinez-arias (1998)
0.3 % Pt/ $\gamma$ -Al <sub>2</sub> O <sub>3</sub>	300-525	0.6-8 % CO	NR	55.4	-	-	Harold and Luss (1987)
Pt/ $\gamma$ -Al <sub>2</sub> O <sub>3</sub>	373-433	0.5 % CO 0.5 % O <sub>2</sub>	110 kPa	-	-1	1	Hoebink et al. (1999)
1 % Pt/ $\gamma$ -Al <sub>2</sub> O <sub>3</sub>	333-400	CO/O <sub>2</sub> = 2	NR	65-90	-	-	Matsushashi et al. (2004)
Pt/SiO <sub>2</sub>	300-500	0.1-10 % CO 0.1-10 % O <sub>2</sub>	0.5-4 cm <sup>3</sup> /s	56	-0.2 ± 0.2	0.9 ± 0.1	Cant et al. (1978)
Pt foil	370-1070	P <sub>CO</sub> = 1.33-6.65x10 <sup>-5</sup> Pa P <sub>O<sub>2</sub></sub> = 1.33-13.3x10 <sup>-5</sup> Pa	1.2-2.6x10 <sup>-4</sup> Pa	30-140 with changing P <sub>CO</sub> / P <sub>O<sub>2</sub></sub>	-	-	Golchet and White (1978)

NR: not reported

**Table 2.2.** Continued

Catalyst	T Range (K)	Reactant Composition	Total Flow Rate or Total Pressure	Ea (kJ/mol)	m	n	Ref.
0.27 % Pt/Fiber Glass	435-625	0.2-2 % CO 0.2-2 % O <sub>2</sub>	NR	-	-0.28	1.07	Nicholas and Shah (1976)
Pt(111)	323-430	CO/O <sub>2</sub> = 1-2	10 Torr	35-71	0	1	Hardacre et al. (1993)
Pt(100)	500-725	P <sub>CO</sub> = 0.5-100 Torr	10-100 Torr	137.5	-1	1	Berlowitz et al. (1988)
	<440	P <sub>O<sub>2</sub></sub> = 1-50 Torr	Torr	54.3	0 to -0.6	1	
Pt thin film	P <sub>O<sub>2</sub></sub> = 0.002 Torr 245-260		NR	36	-	-	Burnett et al. (2004)

NR: not reported

### **2.3. Selective CO Oxidation:**

The studies about the selective CO oxidation mainly focused on the CO conversion and the selectivity. The effects of O<sub>2</sub>/CO ratio, the contact time, and the presence of CO<sub>2</sub> and H<sub>2</sub>O were investigated by different groups.

According to a work was done by Kahlich et al. (1997) T<sub>50</sub> of CO oxidation without hydrogen was found to be around 200°C. In the presence of hydrogen, the ignition temperature decreased by about 30°C to ~170°C. The CO conversion began to increase at ~125°C and after a peak point of 80%, it decreased nearly in a linear manner. These were all summarized in Table 2.3. In addition to that, the selectivity was also showing similar trend like CO oxidation. It started to increase from 25% at 100°C and began to decrease after it reached to a maximum point. As the temperature was increased after 230°C, the selectivity decreased and reached around 20% at 350°C.

Another study was performed by Kim and Lim (2002). The general trend was similar with the study of Kahlich et al. (1997). The CO conversion first increased, then exhibited a maximum and finally decreased with increasing reaction temperature. The selectivity also showed a similar trend with temperature. The temperature for the maximum CO conversion coincided with the minimum temperature for complete conversion of O<sub>2</sub>. The selectivity was mainly dependent on the reaction temperature and the feed compositions but was independent of the catalyst activity and CO conversion.

In a study of Son and Lane (2001), the effect of change in O<sub>2</sub> ratio to CO ratio and the contact time on the CO oxidation and the selectivity of 5% Pt/Al<sub>2</sub>O<sub>3</sub> were observed. They found that CO conversion increased with an increase in O<sub>2</sub> concentration, while the CO selectivity decreased. For the effect of contact time, they examined that the CO conversion improved with

increasing contact time over the entire temperature range and especially at the extremes (at 100<sup>0</sup>C and 250<sup>0</sup>C). Moreover, the O<sub>2</sub> conversion was significantly improved at 100<sup>0</sup>C and the selectivity was only slightly affected up to 250<sup>0</sup>C.

Manasilp and Gulari (2002) worked on 1 and 2% Pt/alumina sol-gel catalysts for selective CO oxidation. They found a similar trend for CO conversion as Kahlich et al. was observed. However, the selectivity remained constant between 110 and 170<sup>0</sup>C and then it started to decrease. They also observed the effect of adding oxygen and water vapor to the reaction mixture to CO conversion and selectivity. As the concentration of the oxygen was increased, they obtained that the conversion of CO increased but selectivity decreased. When they added 10% water to mixture, they found that the CO conversion increased, especially at low temperatures. For low conversion temperatures (110 and 190<sup>0</sup>C), the conversion increased by approximately 10-fold. The change in water concentration did not affect the selectivity of reaction significantly.

In another work Son et al. (2002) studied on two 5% Pt/ $\gamma$ -Al<sub>2</sub>O<sub>3</sub> catalysts which were prepared by standard pretreatment and by a new method of pretreatment, involving saturation with water during reduction. Water-pretreated Pt/ $\gamma$ -Al<sub>2</sub>O<sub>3</sub>, showed higher activity and selectivity over a broad temperature range: 27-200<sup>0</sup>C. Son et al. claimed that the reason for that was the particle size difference between the catalysts prepared by different methods. The analyses showed that small metallic particles (~2 nm) exist on the water pretreatment catalyst, while larger metallic Pt particles (~16 nm) existed on the standard pretreatment catalyst.

Avgouropoulos et al. (2002) observed the effect of the presence of CO<sub>2</sub> and H<sub>2</sub>O on the selective CO oxidation. According to the experiments, it can be

concluded that the catalytic performance of Pt/ $\gamma$ -Al<sub>2</sub>O<sub>3</sub> catalyst seemed to be unaffected by the presence of CO<sub>2</sub>. When both CO<sub>2</sub> and H<sub>2</sub>O were present in the feed, the catalyst was more active than when both of these components were absent from the feed for temperature region lower than 145<sup>0</sup>C. For temperatures higher than 145<sup>0</sup>C, the CO conversion achieved at a given temperature was significantly lower in the presence of H<sub>2</sub>O than in its absence. The presence of the water decreased the selectivity of the catalyst with respect to its absence.

**Table 2.3.** The maximum conversions and selectivities of selective CO oxidation reaction

Catalyst	Pt wt %	M <sub>cat</sub> (g)	Dispersion (%)	Gas Composition	Total Flow Rate (ml/min)	Maximum CO Conversion (%)	Maximum Selectivity (%)	Temp. of Maximum Selectivity (°C)	Ref.
Pt/ $\gamma$ -Al <sub>2</sub> O <sub>3</sub>	0.5	0.1	38	1 % CO 1 % O <sub>2</sub> 75 % H <sub>2</sub> N <sub>2</sub> balanced	120	80	40	230	Kahlich et al. (1997)
				0.5 % O <sub>2</sub>					
				1 % CO, H <sub>2</sub> balanced					
Pt/ $\gamma$ -Al <sub>2</sub> O <sub>3</sub>	5	0.3	NR	0.5 % O <sub>2</sub>	300	55	85	100	Son and Lane (2001)
				1 % O <sub>2</sub>					
				2 % O <sub>2</sub>					
Pt/ $\gamma$ -Al <sub>2</sub> O <sub>3</sub>	1	0.32	60	0.5 % O <sub>2</sub>	100	45	48	215	Kim and Lim (2002)
				1 % CO, 50 % H <sub>2</sub> , He balanced					
				1 % O <sub>2</sub>					
Pt/Al <sub>2</sub> O <sub>3</sub> (sol-gel)	1	0.07	NR	2 % O <sub>2</sub>	40	100	50	200	Manasilp and Gulari (2002)
				1 % CO 1 % O <sub>2</sub> 60 % H <sub>2</sub> He balanced					
				110-170					
Pt/ $\gamma$ -Al <sub>2</sub> O <sub>3</sub>	5	0.05	NR	1 % CO 1.25 % O <sub>2</sub> 50 % H <sub>2</sub> He balanced	100	100	51	161	Avgouropoulos et al. (2002)
				80					

NR: not reported

**Table 2.3.** Continued

Catalyst	Pt wt %	M <sub>cat</sub> (g)	Dispersion (%)	Gas Composition	Total Flow Rate (ml/min)	Maximum CO Conversion (%)	Maximum Selectivity (%)	Temp. of Maximum Selectivity (°C)	Ref.									
Pt/Al <sub>2</sub> O <sub>3</sub>	3	0.1	37	2 % CO 1 % O <sub>2</sub> 70 % H <sub>2</sub> N <sub>2</sub> balanced	100	50	50	280	Marino et al. (2004)									
										Pt/Al <sub>2</sub> O <sub>3</sub>	0.19	NR	1 % CO 1 % O <sub>2</sub> 72 % H <sub>2</sub> 22 % CO <sub>2</sub> N <sub>2</sub> balanced	167	100	56	200	Choi and Stenger (2004)
	1.6					100	47	205										
Pt/γ-Al <sub>2</sub> O <sub>3</sub> Standard Pretreated	5	0.1	33	1 % CO 1 % O <sub>2</sub> H <sub>2</sub> balanced	100	90	45	200-250	Son et al. (2002)									
			41															
Pt/γ-Al <sub>2</sub> O <sub>3</sub> Water Pretreated	0.6	0.112	75	5 % CO 70 % H <sub>2</sub> He balanced	100	58	76	160	Wootsch et al. (2004)									
										2 % O <sub>2</sub>								
										2.5 % O <sub>2</sub>								
										3.75 % O <sub>2</sub>								
				5 % O <sub>2</sub>		98	50	130										

NR: not reported



## CHAPTER 3

### EXPERIMENTAL

#### 3.1. Catalyst Preparation

In this study  $\gamma\text{-Al}_2\text{O}_3$  obtained from Johnson Matthey (65 m<sup>2</sup>/g BET surface area) was used as catalyst support. Platinum was incorporated to  $\gamma\text{-Al}_2\text{O}_3$  support by incipient wetness technique. For this, an appropriate amount of the metal salt  $\text{Pt}(\text{NH}_3)_4\text{Cl}_2 \cdot \text{H}_2\text{O}$  (tetraamine platinum-II-chloride, Johnson Matthey) was dissolved in 2 ml distilled water/g support to bring the samples to incipient wetness. The solution was impregnated onto the support and the final mixture was dried overnight at room temperature and at 25°C for 2 hours. Two sets of 2 % Pt/ $\gamma\text{-Al}_2\text{O}_3$  were prepared and each batch was divided into four portions and each portion was calcined in air at a different temperature for 4 hours unless otherwise indicated. The calcination temperatures were selected as 410, 450, 500 and 600°C.

#### 3.2. Characterization of Catalysts

The metal dispersions of the finished catalysts were measured by a modified H<sub>2</sub> chemisorption experiment. After reduction at 350°C in H<sub>2</sub> under static conditions, the catalysts were cooled down to room temperature under

vacuum. The total and weak hydrogen adsorption isotherms were measured in the pressure range of 1 – 40 Torr at room temperature. The difference between total and weak adsorption isotherms extrapolated to zero pressure was taken as strongly adsorbed H<sub>2</sub> and the dispersion of the Pt was calculated by assuming a 1:1 stoichiometry of H:Pt. The details of the volumetric chemisorption technique and the method of dispersion calculations are given elsewhere (Uner, 2004).

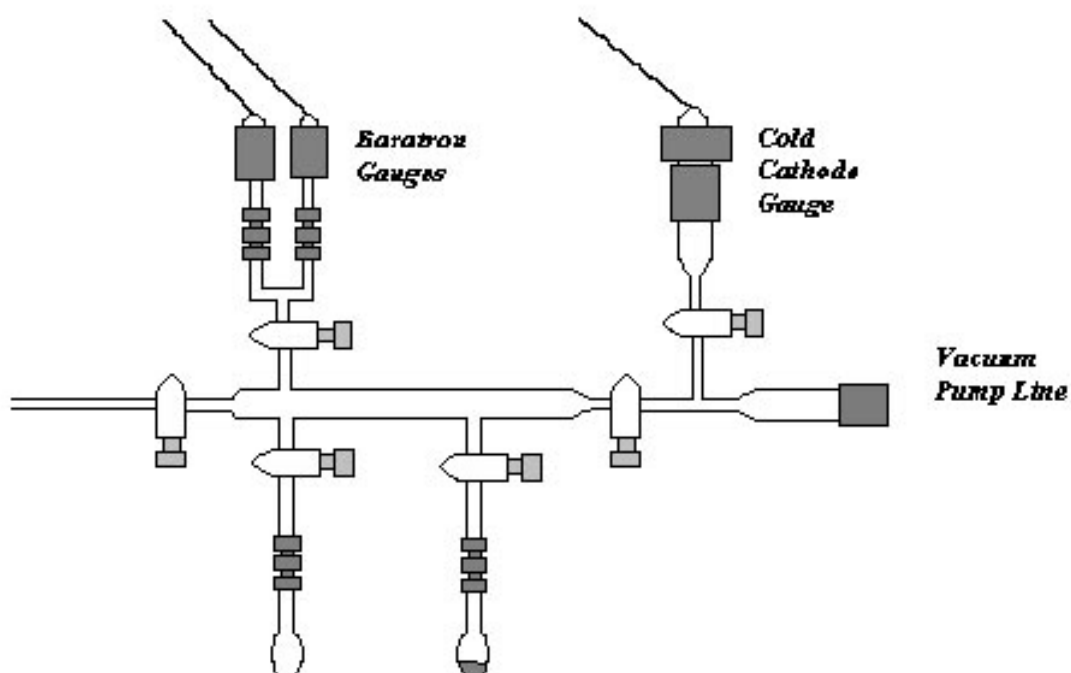


**Figure 3.1:** Home built multi-port high-vacuum Pyrex glass manifold

### 3.3 Activity measurements

The CO oxidation and preferential oxidation of CO performances of these catalysts were tested by using a fixed-bed reactor under atmospheric pressure. In order to do that, a preweighed amount of catalyst was placed in

a pyrex tube of either 5 mm ID or 13 mm ID. When the larger tube was used, 100 mg catalyst diluted with 0.9 g of  $\gamma$ -Al<sub>2</sub>O<sub>3</sub> was placed in the reactor. On the other hand, only 50 mg of catalyst was placed into the glass tube of 5 mm ID. The catalyst beds were supported by quartz wool at both ends for both tubes. The glass reactor was placed inside a temperature controlled (UDC 2300 Universal Digital Controller) tubular furnace (Protherm PTF 12/70/450) for CO oxidation and PROX experiments, respectively. Then the temperature of the furnace was increased from room temperature to reaction temperature at a 1°C/min heating rate (unless otherwise specified) under the flow of feed gases. The temperature of the catalyst bed could be measured by using a thermocouple externally placed on the pyrex tube over the catalyst zone. The internal and external bed temperature calibrations made previously indicated that the external measurement did not bring about much error (Oran, 2001). For CO oxidation in the absence of hydrogen gas, the total flow rate of feed stream was 200 ml/min and it was composed of 5 vol. % CO, 2.5 vol. % O<sub>2</sub>, and the balance helium. The gas flow rates were adjusted by using MKS type 1179A mass-flow controllers. For preferential oxidation of CO experiments, again the total flow rate of feed stream was 200 ml/min and it was composed of 1.6 vol. % CO, 0.8 vol. % O<sub>2</sub>, 20 vol. % H<sub>2</sub> and the balance helium. The product gases were analyzed by using either a gas chromatograph (HP 4890) equipped with a thermal conductivity detector (TCD) or Quadrupole Mass spectrometer (Pfeifer QMS 200). The pyrex tubes of 13 and 5 mm ID were used while the gases were analyzed with gas chromatograph and mass spectrometer, respectively. The conversions were determined from produced CO<sub>2</sub> amounts.

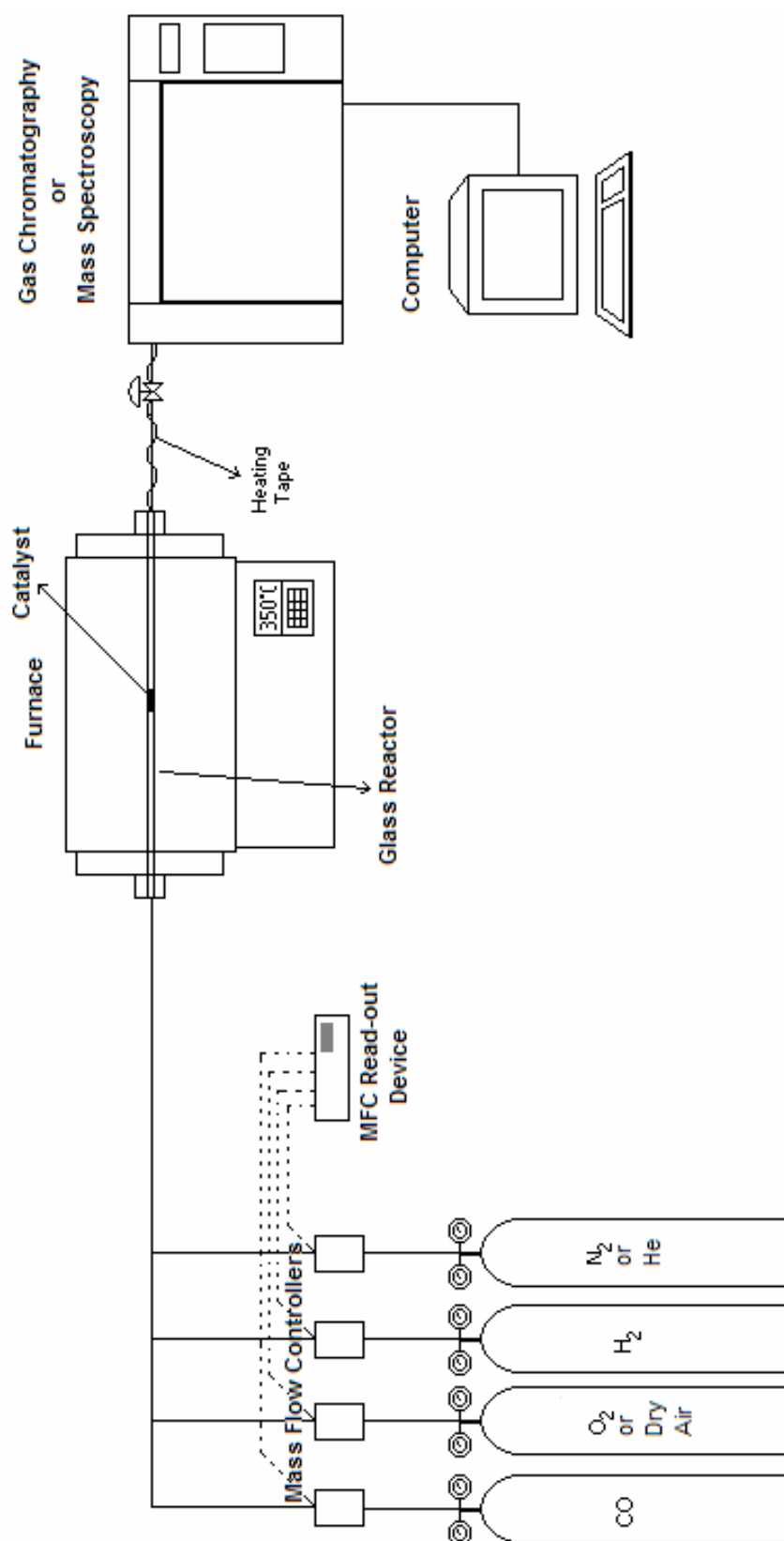


**Figure 3.2** The experimental setup

### **3.4. Isothermal CO Oxidation Reactions**

The reaction orders were determined under isothermal conditions. The experiments were performed at the temperatures where CO conversion is below 5% so that the differential reactor assumption is valid. While keeping the temperature and composition of the one of the reactants constant, the composition of the other reactant was changed. In order to eliminate the oxygen effect during the CO order reactions, the concentration of the oxygen was kept much higher than the concentration of CO and vice versa. The concentration of the CO was changed from 0.7-1.3 % by volume while keeping O<sub>2</sub> at 5.5 % by volume. On the other hand, the concentration of the O<sub>2</sub> was changed from 0.8-1.2 % by volume while keeping the CO at 7 % by volume. As a result, the reaction stoichiometry has spanned the whole range of lean-rich conditions. Experimental conditions such as total feed flow rate and catalyst loading were kept constant at 200 ml/min and 0.1 gram.

## **CHAPTER 4**

### **RESULTS AND DISCUSSION**

#### **4.1. The structure sensitivity of CO oxidation**

The aim of this study is to examine the structure sensitivity of preferential oxidation of CO (PROX) reaction. As it was clearly known that the selective CO oxidation reaction consists of two competitive reactions which are CO oxidation and H<sub>2</sub> oxidation. These reactions occur simultaneously over the surface of the catalysts. Since CO has a poisoning effect for the platinum based catalysts for both CO oxidation and PROX reactions and PROX reaction mainly depends on CO oxidation, the structure sensitivity of CO oxidation reaction has significant importance for the structure sensitivity of preferential oxidation of CO reaction. In recent studies, it was proven that the CO oxidation reaction was a structure sensitive reaction. Therefore, in this part of the study, the CO oxidation performances of the catalysts will be compared with the literature for the structure sensitivity of CO oxidation reaction.

First of all, the catalysts were prepared with the same metal loading but different dispersions. The dispersions of the catalysts were modified by changing the calcination temperatures of catalysts during the preparation. As the calcination temperature was increased, the dispersion of catalysts

decreased and the particle sizes of catalysts increased. If the particle size of the catalysts was changed, the fraction of the low and high coordination atoms on the surface of catalyst could also be changed as it was given in Figure 1.2. It is known that the fraction of low coordination atoms increases with increasing particle size. As it can be seen in Figure 1.2, if it is possible to prepare very large particles, it is also possible to prepare catalysts, nearly free of defect like sites.

#### **4.1.1. Light-off performances of catalysts**

In order to compare the activities of the catalysts with respect to CO oxidation in the absence of hydrogen, CO conversion versus temperature graphs which was also called as light-off curves for four catalysts calcined at different temperatures were plotted and given in Figure 4.1. The effluent gases of reaction were detected by a gas chromatograph. For these experiments, 0.1 grams of catalyst was diluted with 0.9 grams of  $\gamma\text{-Al}_2\text{O}_3$ , placed in 13 mm ID Pyrex reactors and tested. Each catalyst was preconditioned under the flow of 5% CO and balance  $\text{N}_2$  at  $350^\circ\text{C}$  in order to reduce the catalyst. The catalyst bed was cooled down to  $40^\circ\text{C}$  under the same feed conditions after 2 h of preconditioning. By this way, the surface was reduced and saturated with CO, thus steady-state condition was maintained in the beginning of the experiment. Finally reactive gases were fed to the reactor while reactor temperature was gradually increased for  $1^\circ\text{C}/\text{min}$ .

As it can be seen from Figure 4.1, the catalysts exhibited no measurable activity below  $150^\circ\text{C}$ . For all of the catalysts, the conversion of CO did not exceed 30% until the reaction ignited. At ignition temperature (the temperature where the conversion of CO reached to 50%) the conversion

suddenly increased from 30% to 100% within 3-5°C. This phenomenon was caused by the poisoning effect of CO on platinum surfaces. At low temperatures platinum surface is covered by CO, almost completely. Since the surface is saturated with CO, it is poisoned; no oxygen chemisorption can take place and the reaction is inhibited. As the desorption temperature of carbon monoxide is approached and CO starts to empty the active sites; oxygen can find suitable sites to adsorb and reaction proceeds autothermally. Because of that, the conversion of the reaction reached 100% within 3-5°C temperature range.

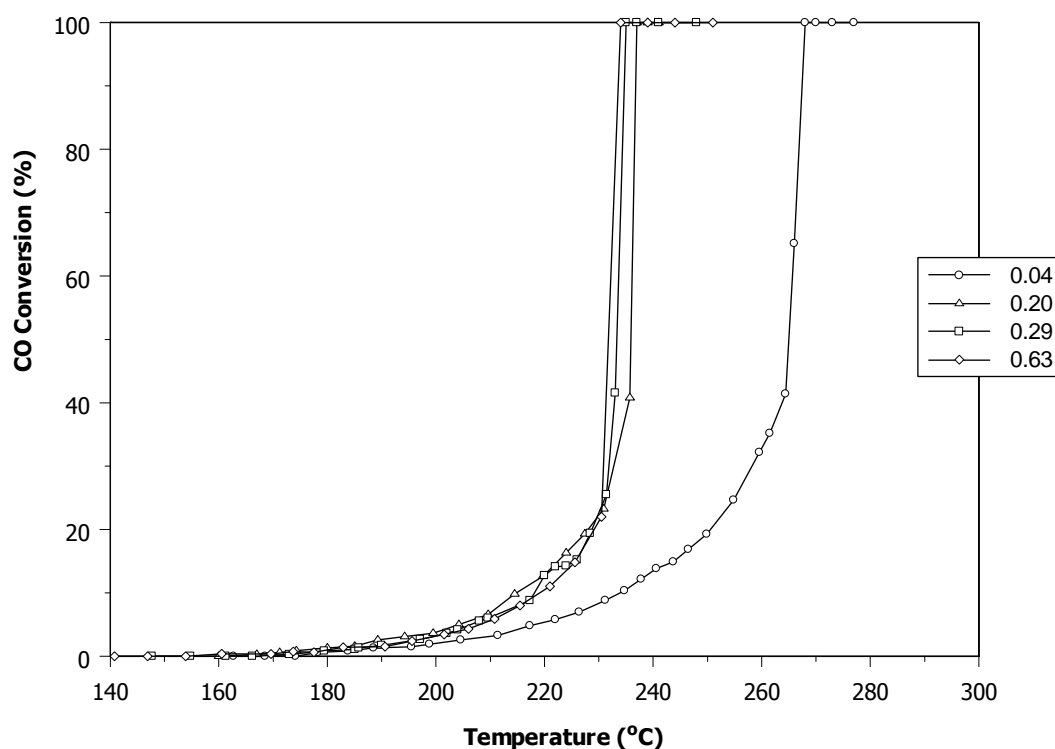


**Figure 4.1** The light-off curves of the catalysts with different dispersions (5% CO, 2.5% O<sub>2</sub> and balance N<sub>2</sub>; Flow rate: 200 ml/min, Catalyst bed: 0.1 g of catalyst diluted by 0.9 g of  $\gamma$ -Al<sub>2</sub>O<sub>3</sub>)

The T<sub>50</sub>'s (the temperature where the conversion of CO reached to 50%) were around 230°C for the samples with dispersions of 0.63, 0.29 and 0.20



and did not show a significant difference. This is reasonable because the order of magnitude of dispersion values of these catalysts is not much different from each other. That result was supported by the data of Gracia et al. (2003). They also found that the light-off plots of catalysts, which dispersions were 0.29 and 0.76, were quite similar.

Although the  $T_{50}$  of high dispersion catalysts were nearly the same, the  $T_{50}$  of the lowest dispersion sample was about 30°C higher than that of the other samples. Since the metal particles formed larger clusters, due to calcination at higher temperatures, the concentration of the edge and corner sites significantly decreased for the samples calcined at higher temperatures (Figure 1.2). In order to infer further judgment, the turnover frequencies, i.e., the ratio of the reaction rate to active site density should be take into consider.

#### **4.1.2. Turnover frequencies of CO oxidation over different catalysts**

In order to clarify the structure sensitivity of any reaction, the turnover frequencies of the catalysts with varying particle size should be compared. If there is any difference between the turnover frequencies of the reaction over the catalysts with varying particle size, it can be concluded that this reaction is structure sensitive. The turnover frequency (TOF) is the ratio of the reaction rate to active site density. The reaction rate of the reaction can be calculated by using the conversion data. The active site density can be obtained by using catalyst metal content and the dispersion values. So, the TOF values can be obtained as the ratio of these two values. As a result, TOF gives how many molecules of  $\text{CO}_2$  are produced per surface platinum atom per unit time for CO oxidation reaction (the calculation procedure was given in Appendix B). Since the data collected from the mass spectrometer could

not be quantitatively calibrated, it was preferred to use arbitrary units instead of  $(\frac{\text{moles}}{\text{g} \cdot \text{atoms} \cdot \text{sec}})$  while the unit of TOF was given.

So, the turnover frequencies of catalysts with different particle sizes were calculated and plotted in Figure 4.2.

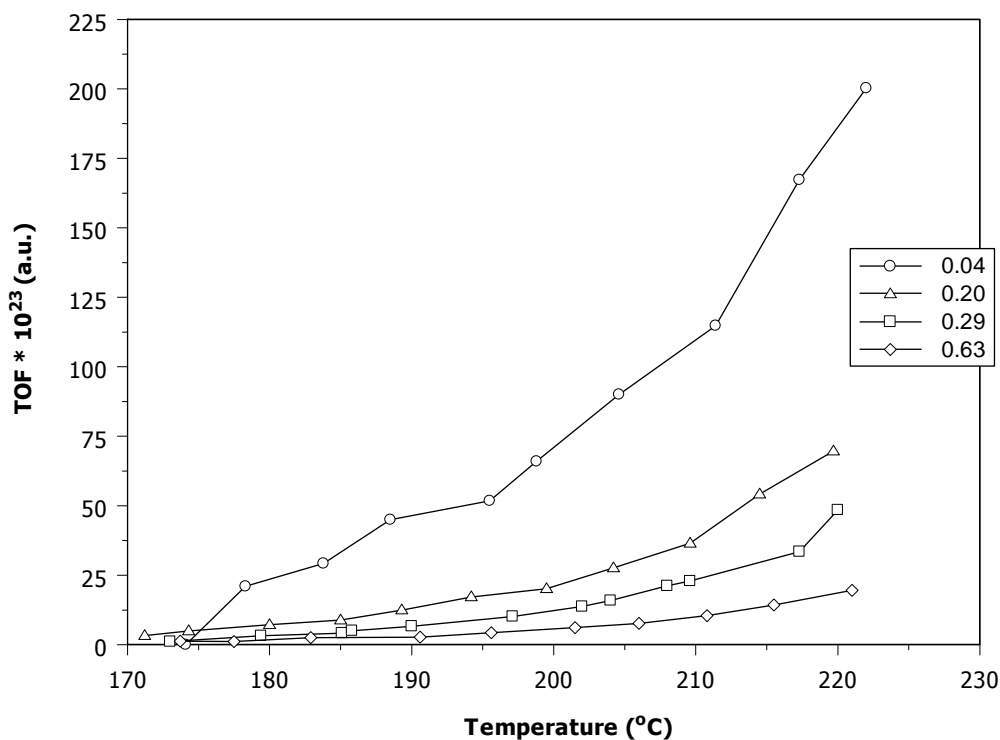


**Figure 4.2** The turnover frequencies of samples with different dispersions with respect to temperature

Although the reaction rate for unit amount of catalysts were similar for three catalysts with dispersions of 0.69, 0.29 and 0.20, the turnover frequencies (the reaction rate per active site density) of catalysts were increasing with increasing particle size, i.e., the activity per surface platinum atom increased with increasing particle size. The catalyst with dispersion of 0.04 had the highest turnover frequency (its TOF is about one order of magnitude higher than that of sample with dispersion of 0.69). A similar trend was found by

Gracia et al. (2003). The turnover frequencies of four catalysts (with dispersions of 0.29, 0.51, 0.63 and 0.76) were increasing with decreasing dispersion value. Gracia et al. (2003) observed that there was an approximately three-fold increase in the TOF as the dispersion decreases from 0.63 to 0.29. That increase was nearly the same for our catalysts. In the study of Zafiris and Gorte (1993), the TOF for 14-nm particle sized catalyst was found to be nearly ten-fold greater than that of catalyst particles with 1.7-nm. So, our data was qualitatively in agreement with the literature.

The difference between the turnover frequencies of catalysts with varying dispersions can be explained by the difference in the relative fraction of low coordination and high coordination platinum atoms on the catalyst particle surface. As it was mentioned before, fractions of Pt atoms at low coordination sites, i.e., corner and edges, decreased while the fraction of atoms on planar faces increased as the crystallite size increased (Figure 1.2, Schimpf, 2002). According to our result, it was found that the turnover frequency was increasing with increasing particle size. Thus, the number of molecules reacting per active site was increasing with increasing particle size. Since the fraction of planar faces increased with increasing particle size, it can be concluded that flat surfaces had a significantly higher CO oxidation activity per surface site compared to low coordination edge and corner atoms. This observation could be supported with the studies performed by using different single crystal platinum catalysts. It was found that CO adsorbed on planar surfaces was more reactive than when adsorbed at step sites (Gland et al., 1983; Szabo et al., 1992; Xu and Yates, 1993). So, it can be said that CO oxidation reaction is faster on planar surfaces with respect to edge and corner sites. It can be concluded that, the CO oxidation reaction is a structure sensitive reaction as it was observed in literature.

### 4.1.3. Apparent activation energies of CO oxidation over different catalysts

Apparent activation energies of CO oxidation reaction on 2% Pt/ $\gamma$ -Al<sub>2</sub>O<sub>3</sub> catalysts were calculated by using the light-off curves. Although plug flow reactor was being used for determining the light-off curves, it was assumed that the reactor behaved as differential reactor for conversions between 0 to 10%. It is assumed that below these conversions axial composition differences are negligible such that the reactor behavior is similar to a CSTR. The ln(rate) vs. 1/T graphs were plotted directly from the light-off curves where conversion was below 10% and the slope of these plots were used to calculate the apparent activation energies of the reactions over the catalysts with different particle sizes. A sample ln(rate) versus 1/T graph and apparent activation energy calculation were given in Appendix B. The calculated apparent activation energies were collected in Table 4.1.

As it can be seen from Table 4.1, the activation energy was decreasing with increasing particle size. Although the sample which dispersion was 0.04 had the lowest activity among other catalysts, the reaction was seemed to face with the weakest activation barrier on this catalyst. The activation energy was varying from 35 to 140 kJ/mol.K in literature, as it was given in Table 2.2. So, our data is quantitatively reasonable. If the results were compared with the data of Zafiridis and Gorte (1993) and Gracia et al. (2003) given in Table 4.1, it could easily be said that our results were qualitatively in agreement with the literature in such a way that the activation energy was decreasing with increasing particle size. As it was said before, the fraction of planar sites on surface of catalyst was increasing with increasing particle size (Figure 1.2). It was given for single crystal catalysts in Table 2.1 that the heat of adsorption of CO was higher at the step and edge sites. So, at corner and edge sites the more strongly adsorbed reactant should overcome an

additional energy barrier to react. The increase in activation energy with decreasing particle size was reasonable since the fraction of corner and edge atoms was increasing with decreasing particle size.

**Table 4.1** The activation energies of CO oxidation reaction with respect to dispersion and particle size of catalysts. The catalysts were tested in a diluted reactor (0.1 g catalyst diluted with 0.9 g  $\gamma$ -Al<sub>2</sub>O<sub>3</sub>)

Pt Particle Size (nm)	Dispersion (%)	Ea (kJ/mol.K)	References
-	0.04	96±2	This Work
-	0.20	107±5	
-	0.29	115±3	
-	0.69	120±3	
14	-	125±12	Zafiris and Gorte (1993)
1.7	-	172±17	
5	0.29	55±1	Gracia et al. (2003)
2	0.63	72±3	
<2	0.76	92±3	

#### 4.1.4. Structure sensitivity of PROX reaction

As it was said before, the aim of this study is to observe the structure sensitivity of selective CO oxidation reaction. Although gas chromatograph could detect CO and CO<sub>2</sub> gases, it could not detect H<sub>2</sub> and H<sub>2</sub>O gases. In order to detect these gases, mass spectrometer was used for the selective CO oxidation reaction product analysis. Due to the equipment change, the light-off experiments performed by using the gas chromatograph were repeated with the same catalysts by using mass spectrometer for verification.

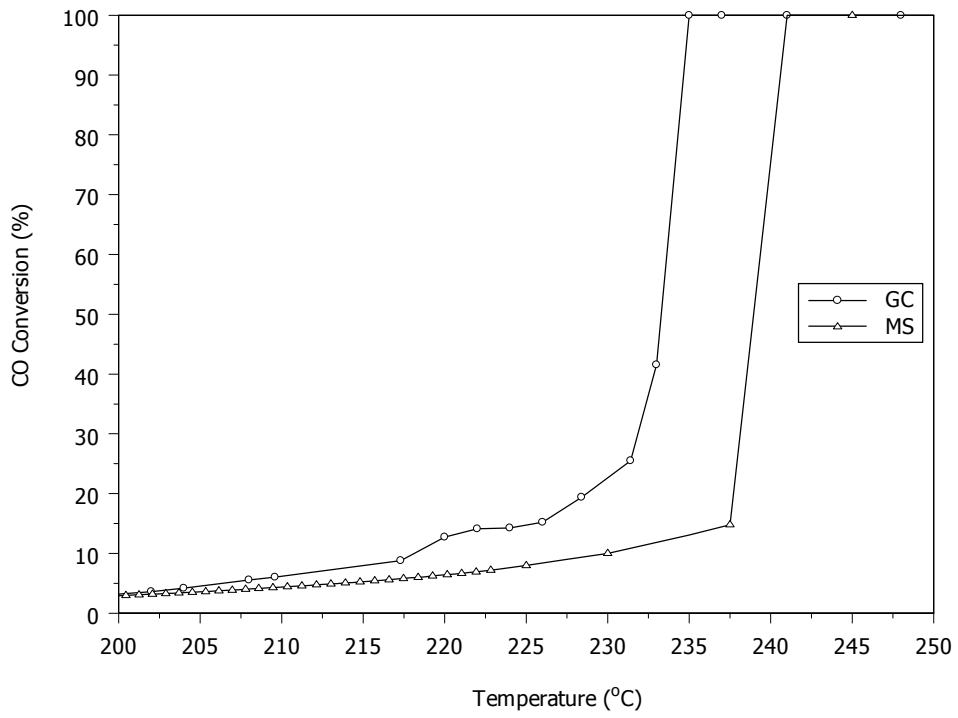
The same experiments were repeated with the same catalysts, however, at this time the catalysts were not diluted with support material and 0.1 grams of 2% Pt/ $\gamma$ -Al<sub>2</sub>O<sub>3</sub> was directly placed into the catalyst bed.

The light-off temperature ( $T_{50}$ ) of each catalyst was compared in order to examine the validity of the data obtained by using mass spectrometer. The  $T_{50}$ 's of all catalysts obtained by using both equipment and the difference between the data were given in Table 4.2.

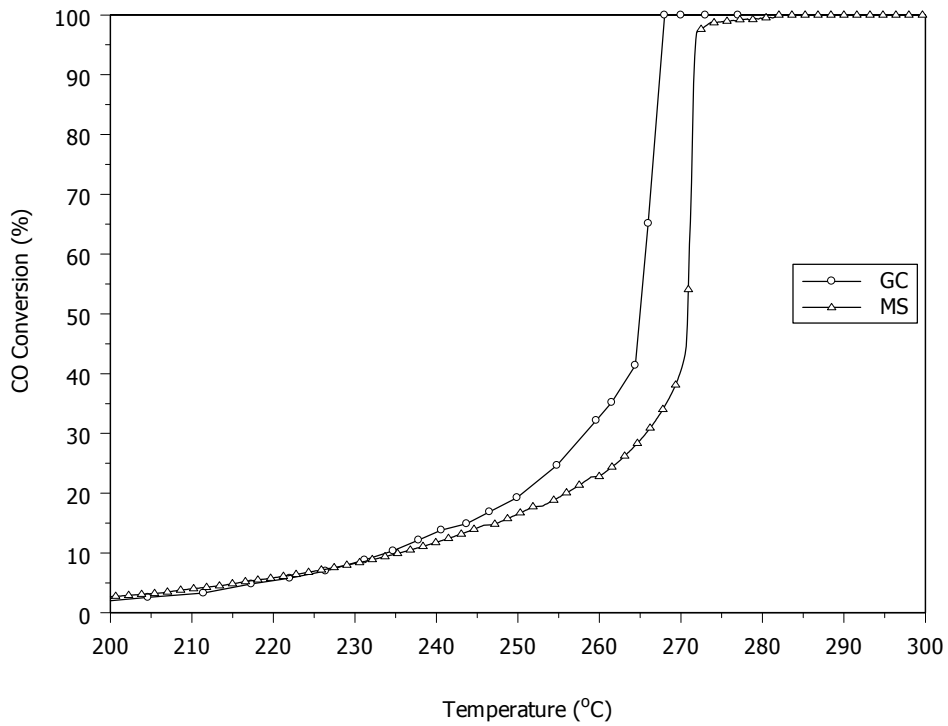
**Table 4.2.** The  $T_{50}$ 's which were obtained by using both GC and MS for all catalysts

<b>Dispersion of the catalysts (%)</b>	<b><math>T_{50}</math> obtained by using GC (°C)</b>	<b><math>T_{50}</math> obtained by using MS (°C)</b>	<b>Difference between two data (°C)</b>
0.04	265	271	6
0.20	236	250	14
0.29	234	240	6
0.63	232	220	-12

The difference between the ignition temperatures of the same catalysts obtained by using two types of systems were considered tolerable. Maximum and minimum differences between the  $T_{50}$ 's were 14 and 6°C, respectively. These graphs were given in Figure 4.3. As such, the results from both systems could be considered comparable.



(a)



(b)

**Figure 4.3** The maximum and minimum differences between  $T_{50}$  data obtained by gas chromatograph and mass spectrometer (a)  $d=0.29$ , (b)  $0.04$

## **4.2. Preferential oxidation of CO (PROX) reaction**

Due to the limited amount of catalysts, new batch of catalysts were prepared and characterized. The dispersions of these catalysts were given in Table 4.3.

### **4.2.1. CO oxidation in the absence of H<sub>2</sub>**

In order to see the effect of hydrogen on the CO oxidation reaction, first the light-off curves were obtained for CO oxidation in the absence of hydrogen and given in Figure 4.4. These experiments were performed with non-diluted catalyst bed (0.05 g of 2% Pt/ $\gamma$ -Al<sub>2</sub>O<sub>3</sub> was used) and the concentration of effluent gases were detected by mass spectrometer.

As it can be seen from Figure 4.4, there were discrepancies between the T<sub>50</sub>'s of the catalysts. The ignition temperatures of the catalysts increased with decreasing dispersion value. The catalyst with greatest particle size had the lowest activity like in previous experiments.

If the T<sub>50</sub>'s of CO oxidation reactions over two batches of catalysts were compared, it can be said that the results about the light-off performances of the catalysts were highly reproducible.



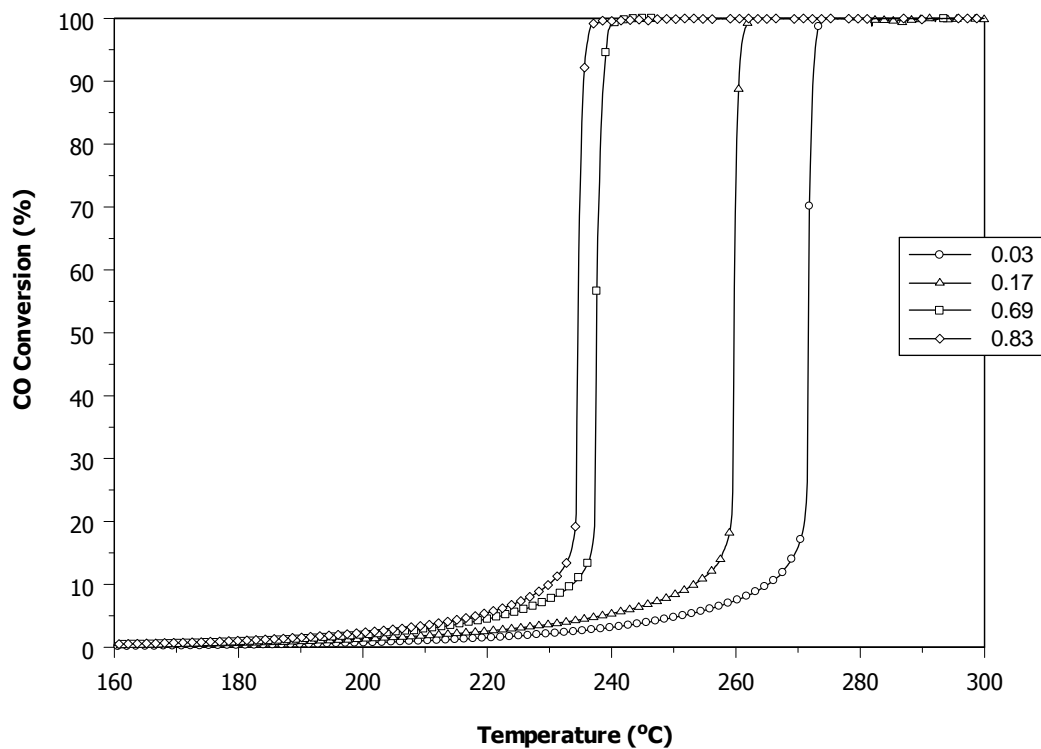


**Figure 4.4** The light-off curves of the catalysts for various dispersions (5% CO, 2.5% O<sub>2</sub> and balance He; Flow rate: 200 ml/min, Catalyst bed: 0.05 g of catalyst)

As it was given in Figure 4.5, the turnover frequency of the catalysts increased with decreasing dispersion. So, this result was qualitatively in agreement with both the previous experiment and the literature.

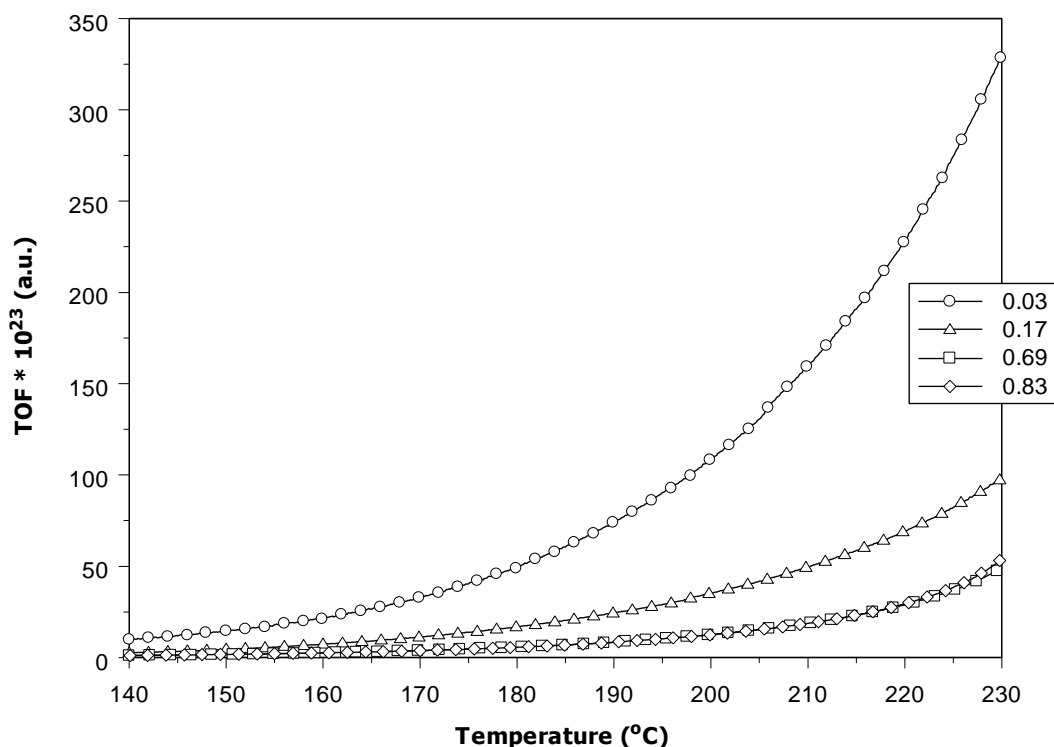


**Figure 4.5** The turnover frequencies of samples with changing dispersions with respect to temperature

#### 4.2.2. CO oxidation in the presence of H<sub>2</sub>

The preferential oxidation of CO reaction in excess hydrogen experiments was investigated by changing the reactor temperature. The oxygen conversion, CO conversion and selectivity with respect to temperature plots were obtained for four catalysts with different particle size. It was tried to examine the structure sensitivity of PROX reaction.

The concentration of oxygen within the catalyst bed drops to zero after a certain temperature for four catalysts when hydrogen was also used in the feed stream (Figure 4.6). The ignition temperature of the reaction increased with decreasing dispersion as it was observed during the CO oxidation in the

absence of hydrogen experiments. However, there was difference between the ignition temperatures of two types of experiments quantitatively. The ignition temperatures of reaction over various catalysts shifted to lower temperatures in the presence of hydrogen. If hydrogen was present in the reaction mixture, the ignition temperatures decreased in the range of 9-55°C as it was given in Table 4.3.

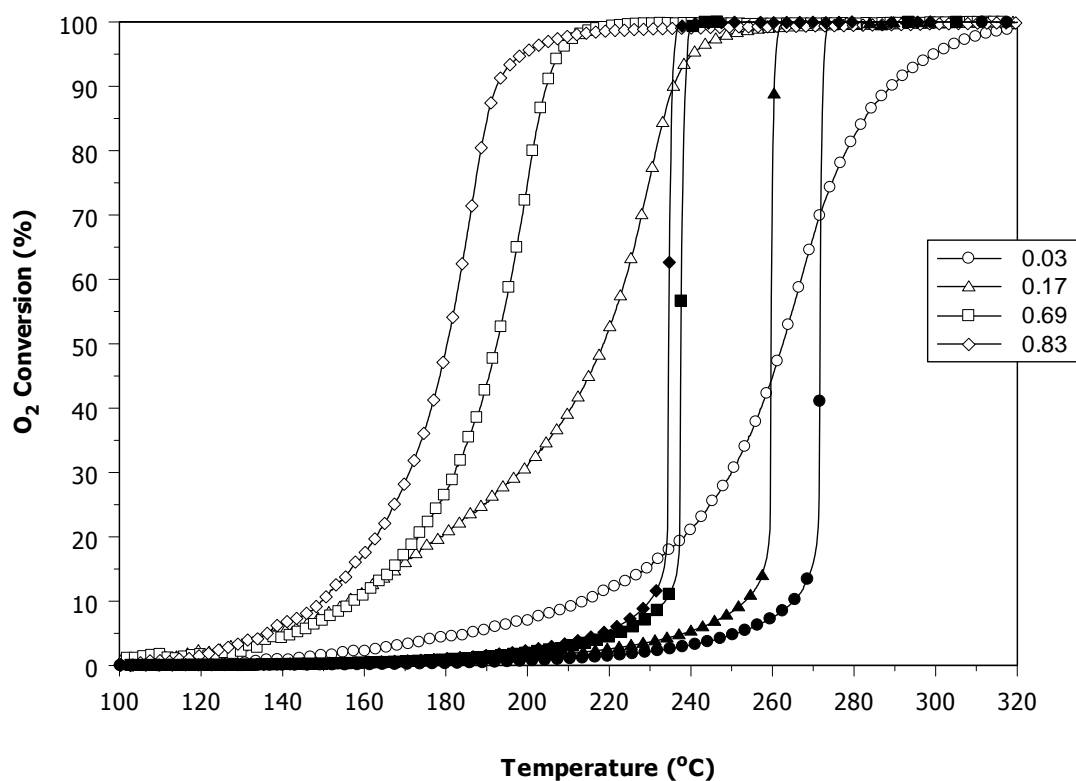


**Figure 4.6** The oxygen conversion of samples with changing dispersions with respect to temperature (The open symbols refer to the reaction of 1.6% CO, 0.8% O<sub>2</sub>, 20% H<sub>2</sub> and balance He; the filled symbols show the reaction of 5%CO, 2.5% O<sub>2</sub> and balance N<sub>2</sub>; Total flow rate: 200 ml/min, Catalyst bed: 0.05 g of catalyst)

**Table 4.3** The  $T_{50}$  of PROX reactions over 2% Pt/ $\gamma$ -Al<sub>2</sub>O<sub>3</sub> catalysts in the presence and absence of hydrogen

<b>Dispersion of Catalyst</b>	<b><math>T_{50}</math> without H<sub>2</sub> (°C)</b>	<b><math>T_{50}</math> with H<sub>2</sub> (°C)</b>	<b>Difference between the <math>T_{50}</math>'s</b>
0.83	235	180	55
0.69	238	192	46
0.17	260	219	41
0.03	272	263	9

The decrease in ignition temperature in the presence of hydrogen was also observed by Kahlich et al. (1997). The ignition temperature of the reaction decreased by about 30°C to ~170°C as it was observed in studies of Oh and Sinkevitch (1993).

The difference between the ignition temperatures was decreasing with decreasing dispersion values. While it was 55°C over the catalyst with dispersion of 0.83, it decreased to 9°C over the catalyst with dispersion of 0.03. The structure sensitivity of hydrogen chemisorption has been established previously (Savargaonkar et al., 1998; Savargaonkar et al., 2002). Our results were consistent with the postulates of Savargaonkar et al. (1998) and Savargaonkar et al. (2002).

The CO conversions for various catalysts in the presence of hydrogen were given in Figure 4.7. At low temperatures no CO consumption was observed for all catalysts as it was observed for experiments without hydrogen. The CO conversion started to increase at a certain temperature and reached a maximum. The maximum CO conversion was around 40% for the entire catalysts with different dispersions. After the peak point, it decreased to

about 25-30% at 350°C. This behavior was observed for all catalysts with different particle size.

In addition to CO conversion, the selectivities of the reaction over different catalysts were also obtained. The selectivity was calculated as the ratio of oxygen consumption for the CO oxidation reaction (to CO<sub>2</sub>) over the total oxygen consumption, which includes the loss due to H<sub>2</sub> oxidation (to H<sub>2</sub>O).

$$\% \text{ of selectivity} = \frac{\Delta O_2^{(\text{CO})}}{\Delta O_2^{(\text{CO})} + \Delta O_2^{(\text{H}_2)}} * 100$$

Nearly an identical trend was observed for the selectivity of CO oxidation reaction (Figure 4.8). Below 100°C, the selectivity was less than 5%. Then it increased and reached maximum points of 35-45% for four different catalysts. Like CO conversion, it decreased to approximately 25-35% when the temperature was increased to 350°C. The temperature for the maximum CO conversion coincided with the minimum temperature for complete conversion of oxygen.

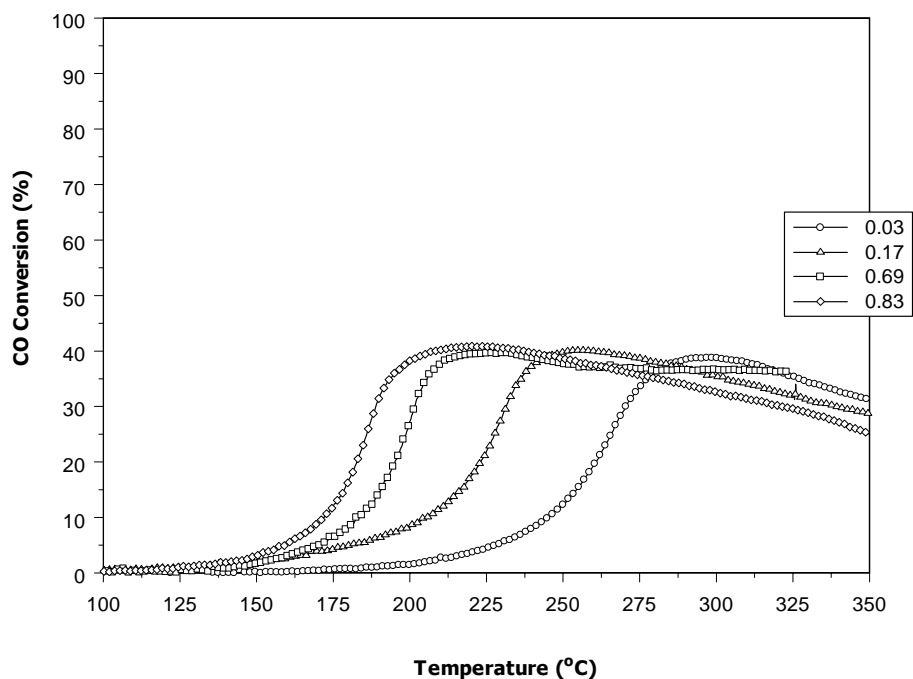


**Figure 4.7** The CO conversion of samples with changing dispersions with respect to temperature (1.6% CO, 0.8% O<sub>2</sub>, 20% H<sub>2</sub> and balance He; Flow rate: 200 ml/min, Catalyst bed: 0.05 g of catalyst)

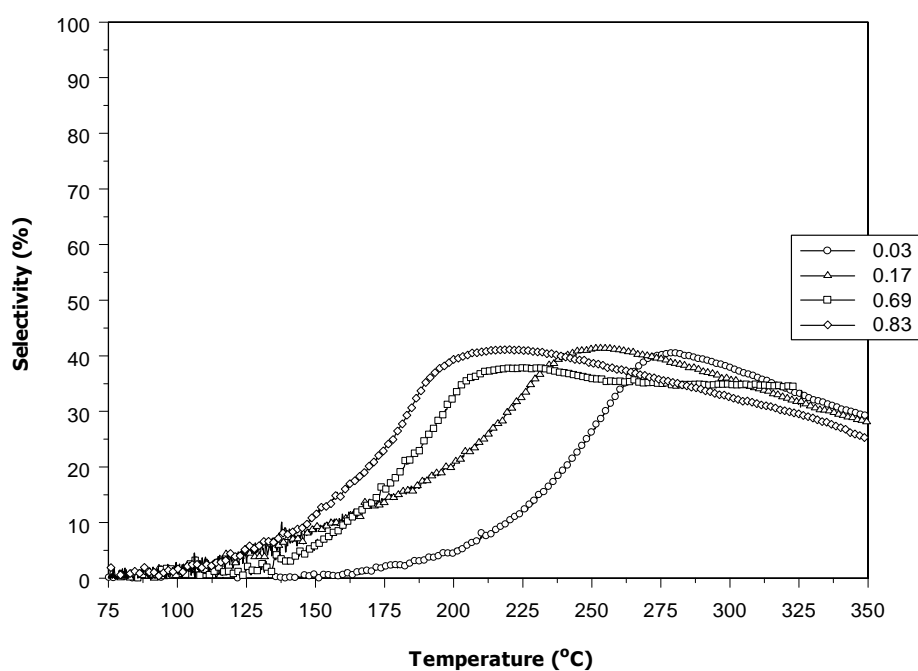


**Figure 4.8** The selectivity for CO oxidation of samples with changing dispersions with respect to temperature

In the literature, the same trend explained above was observed generally (Kahlich et al., 1997; Kim and Lim, 2002; Manasilp and Gulari, 2002; Wootsch et al., 2004; Choi and Stenger, 2004). The CO conversion first increased with increasing reaction temperature, then exhibited a maximum, and finally decreased. The selectivity also showed a similar trend with temperature. In general, below 150°C, it was not seen any CO consumption. The selectivity and CO conversion mainly depend on the O<sub>2</sub>/CO ratio ( $\lambda=2P_{O_2}/P_{CO}$ ). The CO conversion increases with increasing  $\lambda$  and reaches to 100% when  $\lambda$  is greater than 1.5. On the other hand, the selectivity of CO oxidation is decreasing with increasing  $\lambda$ . For instance, in the study of Wootsch et al. (2004), the maximum selectivity decreased from 76% to 50% when  $\lambda$  was increased from 0.8 to 2. In addition to that, the temperature where maximum selectivity was reached was changing for all studies. So, in addition to basic parameters, such as  $\lambda$  and catalyst metal content, there were many variables that could influence the temperature of maximum selectivity.

In this study,  $\lambda$  was used as 1 (stoichiometric amount of CO and O<sub>2</sub> were fed in the reactor). So, firstly it would be more reasonable to compare the CO conversion and selectivity data with the studies which took  $\lambda$  as 1. As it was claimed before, both the maximum CO conversion and selectivity was found to be around 40% for this study. Son and Lane (2001) observed that the CO conversion and selectivity was changing between 40-55% and 42-58%, respectively, between the temperatures of 150 and 250°C. These data was given in Table 2.3, previously. Both CO conversion and selectivity was quite greater than the values obtained in this study. In the study of Kim and Lim (2002), the values were much closer to our experimental data. They found maximum CO conversion and selectivity as 45% and 48%, respectively. In another study, Marino et al. (2004) found that the CO conversion and

selectivity showed a similar trend and the values of them nearly the same after a certain temperature. Both the CO conversion and selectivity increased from 35 to 50% when the temperature was increased from 200 to 300°C. That data was strongly matching with our results. Finally, Wootsch et al. (2004) observed a much higher CO conversion and selectivity with respect to our results. That can be caused by the fraction of CO and O<sub>2</sub> that they used in the feed stream.

Although the CO conversion was much higher than that of our results for studies that used O<sub>2</sub>-rich feed streams, the selectivity values in the literature were close to our data. As it was said before, the CO conversion exceeds 90% as  $\lambda$  is increased to greater than 1 because of the excess oxygen in the gas phase. However, the selectivity cannot exceed 50% for oxygen rich mixtures. So, it can be said that our selectivity data is in accordance with the literature.

As it was claimed before, the CO conversion and selectivity increased, reached a maximum and, then decreased with increasing temperature. CO competes with hydrogen for oxygen in the reaction. Although the hydrogen oxidation occurs even at room temperature in the absence of CO, the reaction is ignited at much higher temperatures in the presence of CO over a platinum catalyst. CO has a poisoning effect for Pt catalysts. It covers the metal surface and inhibits the hydrogen oxidation. In a study about that issue, it was found that the full coverage of CO was observed at temperatures below 200°C for 0.01% CO mixture and 300°C for 1% CO (Dulaurent and Bianchi, 2000). As the temperature was increased, CO was partially desorbed and the coverage of CO decreased. The CO-TPD data of Kahlich et al. (1997) was demonstrating that only ~10% of the initial CO coverage remained on the surface at 250°C. As the hydrogen finds empty sites to adsorb, the hydrogen oxidation can occur. Since the hydrogen



oxidation proceeds much faster than the CO oxidation, decrease in CO conversion and selectivity can be observed after the maximum point. At these temperatures, the oxygen concentration within the catalyst bed drops to zero and oxygen becomes rate-limiting. Therefore, the maximum CO conversion at  $\lambda=1$  could not exceed around 40% for our experiments.

In the low-temperature region, the selectivity increased and showed a maximum. Kahlich et al. (1997) explained this increase by the reduction in hydrogen coverage with increasing temperature. They assumed that H<sub>2</sub> and CO were co-adsorbed on the surface, so that the selectivity should only depend on the ratio between the coverages of H<sub>2</sub> and CO. They thought that the increase in the selectivity at low temperature region caused by the difference between the heats of adsorption of H<sub>2</sub> and CO. The lower adsorption energy of hydrogen ( $\sim 80$  kJ/mol on Pt(111)) (Poelsema et al., 1981) compared to CO ( $\sim 140$  kJ/mol on Pt(111)) (Ertl et al., 1977) led to reduction of the hydrogen coverage with increasing temperature, while CO coverage remained close to saturation. This made  $\Theta_{\text{H}_2}/\Theta_{\text{CO}}$  decrease and thus, an increase of the selectivity could be observed.

The selectivity graphs given in Figure 4.8 showed similar trend for four different catalysts with varying particle size. The selectivity increased, reached a maximum and finally decreased with increasing temperature as it was claimed before. Only difference between the plots was the temperature where the selectivity reached to the maximum. The shapes of the plots were nearly identical excluding the temperature of maximum. At temperatures below 225°C, the selectivity was increasing with increasing dispersion (decreasing particle size). At a certain temperature, the selectivities of high dispersed catalysts were higher than the selectivities of low dispersed catalysts. The catalyst with dispersion of 0.83 had the highest selectivity at 200°C. On the other hand, at temperatures above 265°C, the selectivities of

low dispersed catalysts were higher than those of high dispersed catalysts. Especially, above the temperatures that maximum selectivity obtained for catalyst with dispersion of 0.03 (280°C), the selectivity was increasing with decreasing dispersion. This was due to the difference between the ignition temperatures of the catalysts. Since the ignition temperatures of the high dispersed catalysts were lower than those of the low dispersed ones, the selectivities of them began to decrease at lower temperatures. Thus, higher selectivity for low dispersed catalysts at high temperatures was observed.

As it was explained before, the fractions of high and low coordination atoms are changing with varying dispersion of catalysts. The fraction of planar atoms is increasing with increasing particle size while the fractions of corner and edge atoms decrease (Figure 1.2). It was found in earlier section that the turnover frequency of CO oxidation reaction is increasing with increasing particle size (Figure 4.5). Thus, it was concluded that the CO oxidation reaction is faster on planar sites of the Pt metal surface. According to that conclusion, it was expected that the selective CO oxidation reaction would be a structure sensitive reaction. Since the CO oxidation reaction is faster on planar sites, it would be expected that the selectivity of low dispersed catalysts (with greater particle size) should be higher with respect to high dispersed catalysts. However, it was not found such a trend, in order to say that the selective CO oxidation is structure sensitive according to the results for selectivity obtained in this study.

In literature, there were not many studies investigating the structure sensitivity of selective CO oxidation reaction. Only Son et al. (2002) examined the activity and selectivity of that reaction with varying particle size. They prepared two types of Pt/ $\gamma$ -Al<sub>2</sub>O<sub>3</sub> catalysts with two different pretreatment methods. They observed that water-pretreated catalyst showed higher CO conversion and selectivity over a temperature range of 27-200°C.

In addition to that, according to XRD and TEM analysis, they found that the small metallic Pt particles ( $\sim 2$  nm) existed on the water pretreatment catalyst, while larger metallic Pt particles ( $\sim 16$  nm) existed on the standard pretreatment catalyst. So, they argued that the higher activity and selectivity were caused by the smaller particles on the water pretreated catalyst below  $200^{\circ}\text{C}$ .

To conclude, the CO conversion and selectivity were found to be higher for catalysts with smaller particle size below  $225^{\circ}\text{C}$ , but they were higher for catalysts with larger particle size above  $265^{\circ}\text{C}$ . So, it can be concluded that the selective CO oxidation reaction is not structure sensitive.

## CHAPTER 5

### CONCLUSIONS

In this study, the structure sensitivity preferential oxidation of CO (PROX) was investigated. First, the light-off curves, specific rates and activation energies were observed for CO oxidation reaction in the absence of hydrogen over Pt/ $\gamma$ -Al<sub>2</sub>O<sub>3</sub> catalysts with different particle sizes. The catalysts with the highest dispersion had the highest activity but, the turnover frequency was found to increase with decreasing dispersion of the catalysts. The activation energies of the CO oxidation reaction over various catalysts decreased with increasing particle size. According to these results, it was concluded that our catalysts were qualitatively in agreement with the literature. In addition to CO oxidation to in the absence of hydrogen, the light-off curves and selectivity were observed for preferential oxidation of CO reaction. Again, the activity of the catalysts was increasing with decreasing particle size. Both CO conversion and selectivity first increased with increasing reaction temperature, then exhibited a maximum, and finally decreased. However, both of them did not show any trend for different dispersed catalysts for  $\lambda$  was 1. In order to reach a definite conclusion about the structure sensitivity of selective CO oxidation, the experiments with different  $\lambda$ 's and space times over the same catalysts should be performed.

## RECOMMENDATIONS

In literature, it was shown that although the conversion of CO was increasing with increasing  $\lambda$ , the selectivity did not show much difference. So, the structure sensitivity of selective CO oxidation should be investigated for the conditions where  $\lambda$  is higher than 1. In addition to that, the structure sensitivity of selective CO oxidation can be observed at lower temperatures by increasing the space time. If the space time is increased, ignition temperatures are expected to decrease. So, the mechanism of the reaction can change at lower temperatures. Briefly, the experiments with different  $\lambda$  and space time should be performed in future.

## REFERENCES

Avgouropoulos, G., Ioannides, T., Papadopoulou, C., Batista, J., Hocevar, S., Matralis, H. K., (2002), "A comparative study of Pt/ $\gamma$ -Al<sub>2</sub>O<sub>3</sub>, Au/ $\alpha$ -Fe<sub>2</sub>O<sub>3</sub> and CuO-CeO<sub>2</sub> catalysts for the selective oxidation of carbon monoxide in excess hydrogen", *Catalysis Today*, Vol. 75, pp. 157-167

Berlowitz, P. J., Peden, C. H. F., Goodman, D. W., (1988), "Kinetics of CO oxidation on single-crystal Pd, Pt, and Ir", *Journal of Physical Chemistry*, Vol. 92, pp. 5213-5221

Burnett, D. J., Gabelnick, A. M., Marsh, A. L., Lewis, H. D., Yalisove, S. M., Fischer, D. A., Gland, J. L., (2004), "Defect Enhanced Carbon Monoxide Oxidation at Elevated Oxygen Pressures on a Pt/Al<sub>2</sub>O<sub>3</sub> Thin Film", *Journal of Physical Chemistry B*, Vol. 108, pp.5314-5323

Cant, N. W., Hicks, P. C., Lennon, B. S., (1978), " Steady-state oxidation of carbon monoxide over supported noble metals with particular reference to platinum", *Journal of Catalysis*, Vol. 54, pp. 372-383

Choi, Y., Stenger, H. G., (2004), "Kinetics, simulation and insights for CO selective oxidation in fuel cell applications", *Journal of Power Sources*, Vol. 129, pp. 246–254

Collins, D. M., Spicer, W. E., (1977), "The adsorption of CO, O<sub>2</sub>, and H<sub>2</sub> on Pt: I. Thermal desorption spectroscopy studies", *Surface Science*, Vol. 69, pp. 85-113

Dulaurent, O., Bianchi, D., (2000), "Adsorption isobars for CO on a Pt/Al<sub>2</sub>O<sub>3</sub> catalyst at high temperatures using FTIR spectroscopy: isosteric heat of adsorption and adsorption model", *Applied Catalysis A: General*, Vol. 196, pp. 271-280

Engel, T., Ertl, G., (1982), "The Chemical Physics of Solid Surfaces and Heterogeneous Catalysis", Elsevier Amsterdam, Vol. 4

Engstrom, J. R., Weinberg, W. H., (1988), "Analysis of gas-surface reactions by surface temperature modulation: Experimental applications to the adsorption and oxidation of carbon monoxide on the Pt(110)-(1 × 2) surface ", *Surface Science*, Vol. 201, pp. 145-170

Ertl, G., Neumann, M., Streit, K. M., (1977)," Chemisorption of CO on the Pt(111) surface", *Surface Science*, Vol. 64, pp. 393-410

Gland, J. L., McClellan, M. R., McFeely, F. R., (1983), "Carbon monoxide oxidation on the kinked Pt(321)surface", *Journal of Chemical Physics*, Vol. 79, pp. 6349-6356

Golchet, A., White, J. M., (1978), "Rates and coverages in the low pressure Pt-catalyzed oxidation of carbon monoxide", *Journal of Catalysis*, Vol. 53, pp. 266-279

Gracia, F.J., Bollmann, L., Wolf, E.E., Miller, J.T., Kropf, A.J., (2003), "In situ FTIR, EXAFS, and activity studies of the effect of crystallite size on silica-supported Pt oxidation catalysts", *Journal of Catalysis*, Vol. 220, Iss. 2, pp. 382-391

Hardacre, C., Ormerod, R. M., Lambert, R. M., (1993), "Low temperature carbon monoxide oxidation on Pt(111)-dependence of apparent activation energy on reactant gas composition", *Chemical Physics Letters*, Vol. 206, pp. 171-174

Harold, M. P., Luss, D., (1987), "Use of Multiplicity features for kinetic modeling – CO oxidation on Pt/Al<sub>2</sub>O<sub>3</sub>", *Industrial & Engineering Chemistry Research*, Vol. 26, pp. 2099-2106

Henderson, M. A., Yates, Jr. J. T., (1992), "One-dimensional CO island formation in the coadsorption of H<sub>2</sub> and CO on the steps of Pt(112)", *Surface Science*, Vol. 286, pp. 189-204

Hoebink, J.H.B.J., Nievergeld, A.J.L., Marin, G.B., (1999), "CO oxidation in a fixed bed reactor with high frequency cycling of the feed", *Chemical Engineering Science*, Vol. 54, pp. 4459-4468

Igarashi, H., Fujino, T., Watanabe, M., (1995), "Hydrogen electrooxidation on platinum catalysts in the presence of trace carbon-monoxide", *Journal of Electroanalytical Chemistry*, Vol. 391, pp. 119-123



Kahlich, M. J., Gasteiger, H. A., Behm, R. J., (1997), "Kinetics of the selective CO oxidation in H<sub>2</sub>-rich gas on Pt/Al<sub>2</sub>O<sub>3</sub>", *Journal of Catalysis*, Vol. 171, pp. 93-105

Kim, D. H., Lim, M. S., (2002), "Kinetics of selective CO oxidation in hydrogen-rich mixtures on Pt/alumina catalysts", *Applied Catalysis A: General*, Vol. 224, pp. 27-38

Ladas, S., Poppa, H., Boudart, M., (1981), "The adsorption and catalytic oxidation of carbon monoxide on evaporated palladium particles", *Surface Science*, Vol. 102, pp. 151-171

Luo, J. S., Tobin, R. G., Lambert, D. K., Fisher, G. B., DiMaggio C. L., (1992), "CO adsorption site occupation on Pt(335): a quantitative investigation using TPD and EELS", *Surface Science*, Vol. 274, pp. 53-62

Manasilp, A., Gulari, E., (2002), "Selective CO oxidation over Pt/alumina catalysts for fuel cell applications", *Applied Catalysis B: Environmental*, Vol. 37, pp. 17-25

Marino, F., Descorme, C., Duprez, D., (2004), "Noble metal catalysts for the preferential oxidation of carbon monoxide in the presence of hydrogen (PROX)", *Applied Catalysis B: Environmental*, Vol. 54, pp. 59-66

Martinez-Arias, A., Coronado J. M., Cataluna, R., Conesa, J. C., and Soria, J., (1998), "Influence of mutual platinum-dispersed ceria interactions on the promoting effect of ceria for the CO oxidation reaction in a Pt/CeO<sub>2</sub>/Al<sub>2</sub>O<sub>3</sub> catalyst", *Journal of Physical Chemistry B*, Vol. 102, pp. 4357-4365

Masel, R. I., (1996), "Principles of adsorption and reaction on solid surfaces", Wiley Series in Chemical Engineering

Matsushashi, H., Nishiyama, S., Miura, H., Eguchi, K., Hasegawa, K., Iizuka, Y., Igarashi, A., Katada, N., Kobayashi, J., Kubota, T., Mori, T., Nakai, K., Okazaki, N., Sugioka, M., Umekio, T., Yazawa, T., Lu, D., (2004), "Effect of preparation conditions on platinum metal dispersion and turnover frequency of several reactions over platinum-supported on alumina catalysts", Applied Catalysis A: General, Vol. 272, pp. 329-338

McCabe, R. W., Schmidt, L. D., (1977), "Binding states of CO on single crystal planes of Pt", Surface Science, Vol. 66, pp. 101-124

McCarthy, E., Zahradnik, J., Kuczynski, G. C., Carberry, J. J., (1974), "Some unique aspects of CO oxidation on supported Pt", Journal of Catalysis, Vol. 39, pp. 29-35

McClellan, M. R., Gland, J. L., McFeely, F. R., (1981), "Carbon monoxide adsorption on the kinked Pt(321) surface", Surface Science, Vol. 112, pp. 63-77

Muraki, H., Matunaga, S., Shinjoh, H., Wainwright, M. S., Trimm, D. L., (1991), "The effect of steam and hydrogen in promoting the oxidation of carbon monoxide over a platinum on alumina catalyst", Journal of Chemical Technology and Biotechnology, Vol. 52, pp. 415-424

Nibbelke, R. H., Campman, M. A. J., Hoebink, J. H. B. J., Marin, G. B., (1997), "Kinetic study of the CO oxidation over Pt/ $\gamma$ -Al<sub>2</sub>O<sub>3</sub> and Pt/Rh/CeO<sub>2</sub>/ $\gamma$ -Al<sub>2</sub>O<sub>3</sub> in the presence of H<sub>2</sub>O and CO<sub>2</sub>", Journal of Catalysis, Vol. 171, pp. 358-373

Nicholas, D. M., Shah, Y. T., (1976), "Carbon monoxide oxidation over a platinum-porous fiber glass supported catalyst", *Ind. Eng. Chem.*, Vol. 15, pp. 35-40

Oh, S. H., Sinkevitch, R. M., (1993), "Carbon monoxide removal from hydrogen-rich fuel cell feed streams by selective catalytic oxidation", *Journal of Catalysis*, Vol. 142, pp. 254-262

Oran, U., (2001), "Effect of cerium dioxide on carbon monoxide oxidation reaction mechanism over Pt/ $\gamma$ -Al<sub>2</sub>O<sub>3</sub> catalyst", MS. Thesis, Middle East Technical University, Ankara, Turkey

Poelsema, B., Palmer, R. L., Comsa, G., (1981), "The interaction of hydrogen with platinum(s)-9(111)  $\times$  (111) studied with helium beam diffraction", *Surface Science*, Vol. 111, pp. 519-544

Poelsema, B., Palmer, R. L., Comsa, G., (1984), "A thermal He scattering study of CO adsorption on Pt(111)", *Surface Science*, Vol. 136, pp. 1-14

Savargaonkar, N., Narayan, R. L., Pruski, M., Uner, D. O., King, T. S., (1998), "Structure Sensitive Hydrogen Adsorption: Effect of Ag on Ru/SiO<sub>2</sub>Catalysts", *Journal of Catalysis*, Vol. 178, Iss. 1, pp. 26-33

Savargaonkar, N., Uner, D., Pruski, M., King, T. S., (2002), "Kinetics of hydrogen adsorption and desorption on silica supported Pt, Rh and Ru catalysts studied by solid state <sup>1</sup>H-NMR", *Langmuir*, Vol. 18, pp. 4005-4009

Schimpf, S., Lucas, M., Mohra, C., Rodemerck, U., Brückner, A., Radnik, J., Hofmeister, H., Claus, P., (2002), "Supported gold nanoparticles: in-depth catalyst characterization and application in hydrogenation and oxidation reactions", *Catalysis Today* Vol. 72, pp. 63–78

Seebauer, E. G., Kong, A. C. F., Schmidt, L. D., (1986), "Adsorption and desorption of NO, CO and H<sub>2</sub> on Pt(111): Laser-induced thermal desorption studies", *Surface Science*, Vol. 176, pp. 134-156

Siddiqui, H. R., Guo, X., Chorkendorff, I., Yates, Jr. J. T., (1987), "CO adsorption site exchange between step and terrace sites on Pt(112)", *Surface Science*, Vol. 191, pp. L813-L818

Son, I. H., Lane, A. M., (2001), "Promotion of Pt/ $\gamma$ -Al<sub>2</sub>O<sub>3</sub> by Ce for preferential oxidation of CO in H<sub>2</sub>", *Catalysis Letters*, Vol. 76, pp. 151-154

Son, I. H., Shamsuzzoha, M., Lane, A. M., (2002), "Promotion of Pt/ $\gamma$ -Al<sub>2</sub>O<sub>3</sub> by new pretreatment for low-temperature preferential oxidation of CO in H<sub>2</sub> for PEM fuel cells", *Journal of Catalysis*, Vol. 210, pp. 460-465

Strohl, J, King, T. S., Personal Communication

Szabo, A., Henderson, M. A., Yates, Jr. J. T., (1992), "Oxidation of CO by oxygen on a stepped platinum surface: Identification of the reaction site", *Journal of Chemical Physics*, Vol. 96, pp. 6191-6202

Uner, M., (2004), "Adsorption calorimetry in supported catalyst characterization: adsorption structure sensitivity on Pt/ $\gamma$ -Al<sub>2</sub>O<sub>3</sub>", MS. Thesis, Middle East Technical University, Ankara, Turkey

Wang, H., Tobin, R. G., Lambert, D. K., Fisher, G. B., Dimaggio, C. L., (1995), " H-CO interactions on the terraces and steps of a stepped Pt surface", Surface Science, Vol. 330, pp. 173-181

Winkler, A., X. Guo, H. R. Siddiqui, P. L. Hagans and J. T. Yates, Jr., (1988), "Kinetics and energetics of oxygen adsorption on Pt(111) and Pt(112)- A comparison of flat and stepped surfaces ", Surface Science, Vol. 201, pp. 419-443

Wootsch, A., Descorme, C., Duprez, D., (2004), "Preferential oxidation of carbon monoxide in the presence of hydrogen (PROX) over ceria-zirconia and alumina-supported Pt catalysts", Journal of Catalysis, Vol. 225, pp. 259-266

Xu, J., Yates, Jr. J. T., (1993), "Catalytic oxidation of CO on Pt(335): A study of the active site", Journal of Chemical Physics, Vol. 99, pp. 725-732

Yamanaka, T., Moise, C., Matsushima, T., (1997), "Reaction site switching in carbon monoxide oxidation on platinum (113): A spatial distribution study of desorbing product", Journal of Chemical Physics, Vol. 107, pp. 8138-8146

Zafiridis, G. S., Gorte, R. J., (1993), "CO Oxidation on Pt/ $\gamma$ -Al<sub>2</sub>O<sub>3</sub>(0001): Evidence for Structure Sensitive", Journal of Catalysis, Vol. 140, pp. 418-423

## **APPENDIX A**

### **Volumetric Chemisorption**

It is important to know the active site density of a catalyst to be able to make a comparison between catalysts under consideration. The active site density for each catalyst was obtained by using volumetric hydrogen adsorption method. In this method, total and weak chemisorption uptake over a catalyst is measured and the difference between total and weak H<sub>2</sub> adsorbed amount gives the surface active site concentration. Using the surface active site concentration, we can calculate the dispersion of a catalyst which is defined as the ratio of number of surface atoms to the number of total atoms of active metal. Figure A.1 shows H<sub>2</sub> uptake as a function of equilibrium pressure for the catalyst calcined at 410°C (The results of the adsorption experiments of other catalysts are given in Appendix).

The dispersion values of two sets of catalysts are given in Table A.1. It can be seen from the table that as the calcination temperature and duration was increased, the dispersion value of catalysts were decreasing. The calcination temperature and duration is directly affecting the mobility of the platinum atoms on the surface of alumina. As the mobility of the platinum atoms is increasing with increasing temperature and duration, the sintering process goes faster and the particles with higher sizes would be obtained. So, the

ratio of metal atoms exposed to the gas phase to total atoms (dispersion) will decrease.

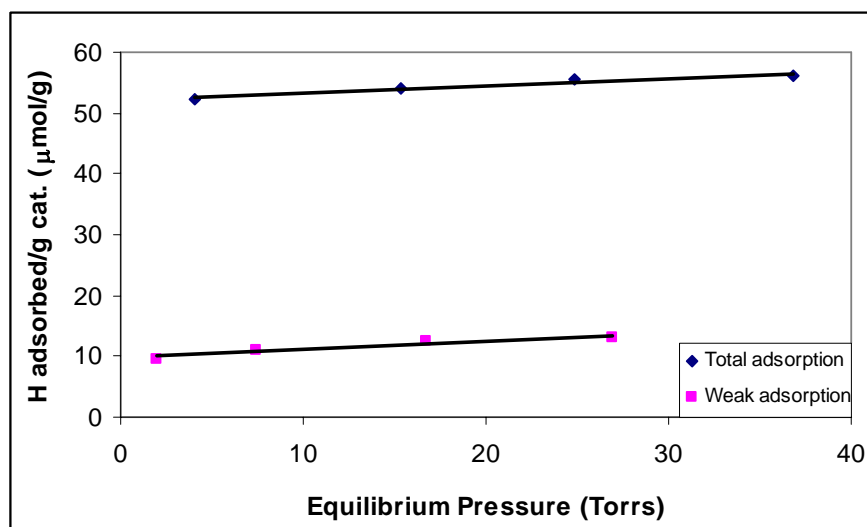


**Figure A.1.** H<sub>2</sub> adsorption isotherm of 2% Pt/γ-Al<sub>2</sub>O<sub>3</sub> with dispersion of 0.83

**Table A.1.** Dispersion values of 2% Pt/Al<sub>2</sub>O<sub>3</sub> calcined at different temperatures and durations

	Calcination Temperature (°C)	Dispersion	Approximate Particle Diameter (Å)	Distance Between the Clusters on the Surface (Å)
<b>Set 1</b>	410	0.63	-	-
	450	0.29	-	-
	500	0.20	-	-
	600	0.04	-	-
<b>Set 2</b>	410	0.83	14.56	75.73
	450	0.76	-	-
	500	0.69	17.97	106.04
	600	0.17	88.50	1276.22
	600*	0.03	637.12	25928.60

\* This catalyst was calcined at 600°C for 11 hours

In order to see the interaction between the clusters existing on the surface of the catalysts, the distances between the clusters were calculated for different catalysts, theoretically. The calculations were performed by using the data given in the study of Strohl and King. The clusters were assumed to be spherical in shape in order to find the projectional area of the cluster during the calculations. In addition to that, the distance between all the clusters was assumed to be equal. First, the diameter of the cluster was obtained by using the dispersion data. Then, the total number of clusters was obtained by using number of surface atoms of a cluster and the total number of platinum atoms exposed to the surface. Finally, the distance between the clusters were calculated by using, the diameter of cluster, the total number of clusters and the total surface area of support material for a certain amount of catalyst.



## APPENDIX B

### Calculations

#### a) Reaction Rate Calculation

As the conversion versus temperature graphs were plotted for the catalysts calcined at different temperatures, we could be able to calculate the reaction rates and activation energies for these catalysts. Although plug flow reactor is being used for the light-off curves, we assumed that the reactor was behaving as differential reactor for conversions between 0 to 10%. So, the reaction rates were calculated for each conversion according to this assumption. The equation used can be given as:

$$\frac{dN_{CO}}{dt} = F_{CO_0} - F_{CO} - (r_{CO} \cdot m_{cat}) \quad (1)$$

Since we assume that the process is at steady state,  $\frac{dN_{CO}}{dt} = 0$

and the equation (1) becomes;

$$r_{CO} = \frac{F_{CO_0} - F_{CO}}{m_{cat}} \quad (2)$$

$$X_{CO} = \frac{F_{CO_0} - F_{CO}}{F_{CO_0}} \quad (3)$$

If equations (2) and (3) is combined, the reaction rate is obtained as;

$$r_{CO} = \frac{F_{CO_0} \cdot X_{CO}}{m_{cat}} \quad (4)$$

where  $F_{CO_0}$  : initial molar flow rate of CO gas  
 $X_{CO}$  : conversion  
 $m_{cat}$  : weight of the catalyst placed into the reactor

### b) Turnover Frequency Calculation

Turnover frequency is the ratio of reaction rate to the active site density. As it was shown previously, the reaction rate was:

$$r_{CO} = \frac{F_{CO_0} \cdot X_{CO}}{m_{cat}}$$

The active density can be calculated by using metal content of catalyst and dispersion.

$$SD = \frac{m_{cat} \cdot W_{Pt} \cdot d \cdot N_{Av}}{M_{Pt}}$$

$$TOF = \frac{r_{CO}}{SD} = \frac{F_{CO_0} \cdot X_{CO} \cdot M_{Pt}}{(m_{cat})^2 \cdot W_{Pt} \cdot d \cdot N_{Av}} \quad \left( \frac{moles}{g \cdot atoms \cdot sec} \right)$$

### c) Apparent Activation Energy Calculation

The power law type reaction rate and Arrhenius equation was used for activation energy calculation.

$$(r_{CO_2}) = k(P_{CO})^a \cdot (P_{O_2})^b$$

By taking the natural logarithm of both sides of the equation

$$\ln(r_{CO_2}) = \ln(k) + \ln[(P_{CO})^a \cdot (P_{O_2})^b]$$

As rate constant is assumed to be Arrhenius type;

$$k = k_0 \cdot e^{\frac{(-E_a)}{R \cdot T}}$$

$$\ln(r_{\text{CO}_2}) = \left(-\frac{E_a}{R}\right)\left(\frac{1}{T}\right) + \ln[k_0 \cdot (P_{\text{CO}})^a \cdot (P_{\text{O}_2})^b]$$

According to this equation, if  $\ln(r_{\text{CO}_2})$  versus  $\left(\frac{1}{T}\right)$  graph is plotted, the slope

of this plot will be equal to  $\left(-\frac{E_a}{R}\right)$ . So, the activation energies can be

calculated by using the slope data. A sample  $\ln(r_{\text{CO}_2})$  vs.  $\left(\frac{1}{T}\right)$  plot was

shown in Figure B.1.

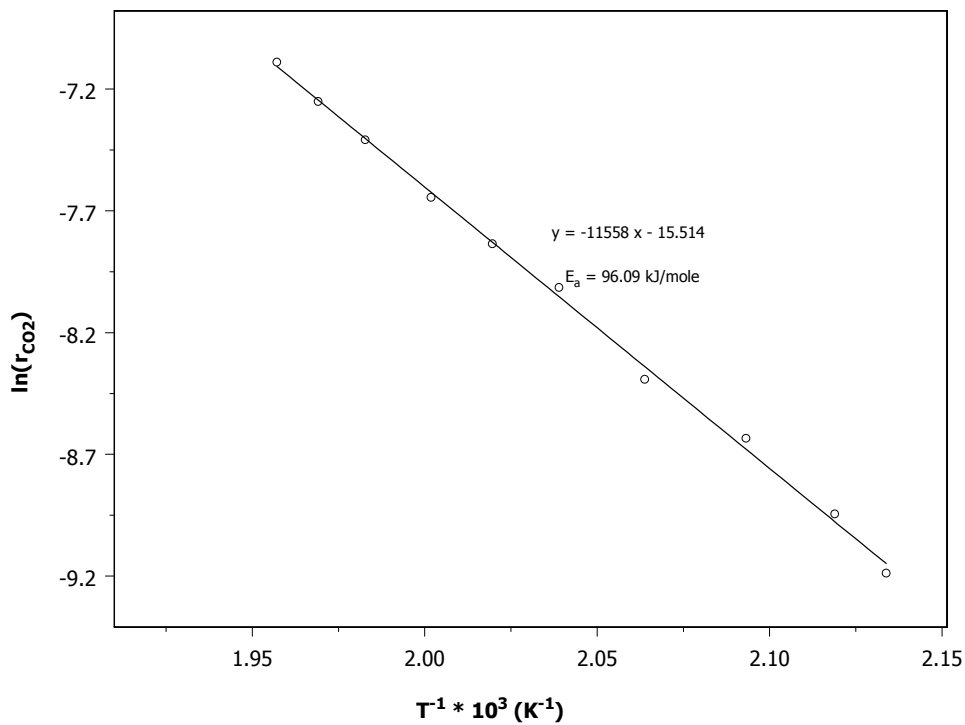


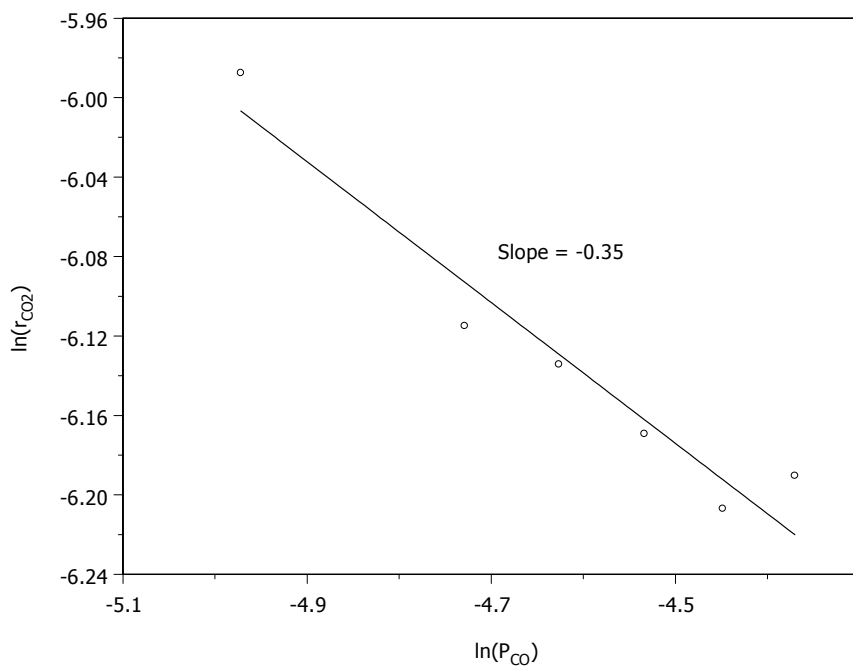
**Figure B.1**  $\ln(\text{rate})$  vs.  $T^{-1}$  plot of 2% Pt/ $\text{Al}_2\text{O}_3$  catalysts which dispersion is 0.04 (5% CO, 2.5%  $\text{O}_2$  and balance  $\text{N}_2$ ; Flow rate: 200 ml/min, Catalyst bed: 0.1 g of catalyst diluted by 0.9 g of  $\gamma\text{-Al}_2\text{O}_3$ )

#### **d) Reaction Orders**

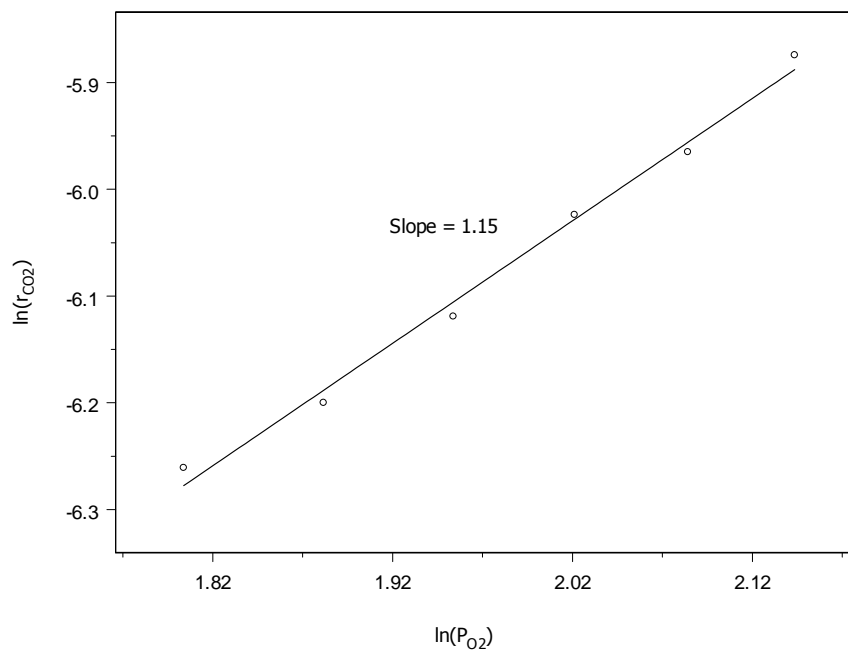
In addition to these, the reaction order of the CO oxidation reaction in the absence of hydrogen was also calculated. The reaction orders could be calculated by using the power law type reaction rate, which was shown before.

$$\ln(r_{\text{CO}_2}) = \ln(k) + \ln[(P_{\text{CO}})^a \cdot (P_{\text{O}_2})^b]$$

In order to find  $a$  (the order of CO), while keeping the temperature and the partial pressure of oxygen constant, the partial pressure of CO was changed. Then,  $\ln(r_{\text{CO}_2})$  versus  $\ln(P_{\text{CO}})$  was plotted and the slope of this graph directly gave the CO order. By following the same procedure, while keeping the temperature and the partial pressure of CO constant, the partial pressure of the  $\text{O}_2$  was changed and the order of  $\text{O}_2$  ( $b$ ) was obtained by plotting  $\ln(r_{\text{CO}_2})$  versus  $\ln(P_{\text{O}_2})$ . Since the temperature was kept constant, the rate constant ( $k$ ) was not changed. The sample plots for the reaction orders of CO and oxygen for the catalyst with dispersion of 0.63 were given in Figure B.1.



(a)



(b)

**Figure B.2** The reaction orders of the reaction over the catalyst with dispersion of 0.63 (a) CO order,  $P_{O_2} = 41.5$  Torr and  $P_{CO} = 5.3-9.6$  Torr ; (b)  $O_2$  order,  $P_{CO} = 55.4$  Torr and  $P_{O_2} = 6.1-8.5$  Torr

## APPENDIX C

### Isothermal CO oxidation performances of 2% Pt/ $\gamma$ -Al<sub>2</sub>O<sub>3</sub> catalysts

The reaction orders were estimated under differential reactor assumption. The calculation of reaction orders were given in Appendix part. Carbon monoxide and oxygen orders were estimated at constant temperature over a narrow range of CO and oxygen partial pressures. The reaction orders of carbon monoxide and oxygen gases were tabulated in Table C.1.

**Table C.1** The reaction orders of CO and O<sub>2</sub> for CO oxidation reaction

Dispersion of Catalysts Set 1	Experiment Temperature for CO (°C)	The order of CO	Experiment Temperature for O <sub>2</sub> (°C)	The order of O <sub>2</sub>
0.63	130	-0.36±0.04	173	1.15±0.05
0.29	155	-0.50±0.06	188	1.15±0.06
0.20	158	-0.41±0.05	170	1.04±0.02
0.04	164	-0.52±0.06	190	0.95±0.05

According to the isothermal experiments, the reaction order of CO was varying from -0.4 to -0.5 and for oxygen it was approximately 1. The different results about the orders of CO and oxygen over various catalysts were given in Table 2.2. The CO order was found to be changing between -1.5 and 0. In addition to that, the oxygen order was generally found to be 1. So, it can be concluded that the reaction orders of CO and O<sub>2</sub> for CO oxidation reaction were approximately -0.5 and 1.0, respectively, according

to our results. It could easily be said that there was no significant difference between the reaction orders of the reaction over various catalysts with different particle sizes. Thus, it can be assumed that CO oxidation reaction mechanism did not change over 2% Pt/ $\gamma$ -Al<sub>2</sub>O<sub>3</sub> catalysts with different dispersions.